JACS
JOURNAL OF THE AMERICAN CHEMICAL SOCIETY
Article
pubs.acs.org/JACS

Interdigitated Hydrogen Bonds: Electrophile Activation for Covalent Capture and Fluorescence Turn-On Detection of Cyanide

Junyong Jo, András Olasz, Chun-Hsing Chen, and Dongwhan Lee*

Department of Chemistry, Indiana University, 800 East Kirkwood Avenue, Bloomington, Indiana 47405, United States

Supporting Information

ABSTRACT: Hydrogen-bonding promoted covalent modifications are finding useful applications in small-molecule chemical synthesis and detection. We have designed a xanthene-based fluorescent probe **1**, in which tightly held acylguanidine and aldehyde groups engage in multiple intramolecular hydrogen bonds within the concave side of the molecule. Such an interdigitated hydrogen bond donor−acceptor (HBD−HBA) array imposes significant energy barriers ($\Delta G^{\ddagger}$ = 10−16 kcal mol^{-1}) for internal bond rotations to assist structural preorganization and effectively polarizes the electrophilic carbonyl group toward a nucleophilic attack by CN^- in aqueous environment. This covalent modification redirects the de-excitation pathways of the cyanohydrin adduct **2** to elicit a large (>7-fold) enhancement in the fluorescence intensity at λ_{max} = 440 nm. A remarkably faster (> 60-fold) response kinetics of **1**, relative to its *N*-substituted (and therefore "loosely held") analogue **9**, provided compelling experimental evidence for the functional role of HBD−HBA interactions in the "remote" control of chemical reactivity, the electronic and steric origins of which were investigated by DFT computational and X-ray crystallographic studies.

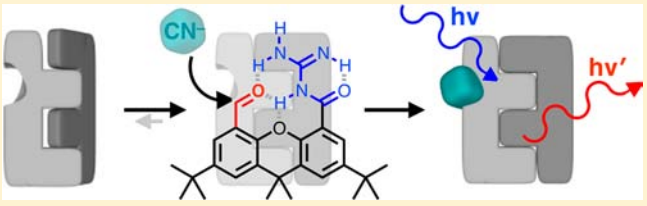

INTRODUCTION

Activation of substrates in enzymatic reactions often proceeds via polarization of scissile chemical bonds.[1] Coordination of metal ions to the Lewis basic functional group is one strategy to achieve this goal.[2] Alternatively, hydrogen bond donor (HBD) groups presented by the inner surface of enzyme active sites can participate in conceptually parallel processes by promoting the reactivity of electrophilic substrates.[3] The oxyanion hole in the serine protease active sites is one prominent example.[1,4] Here, multiple N−H groups from the polypeptide backbone bind and properly orient the substrate carbonyl group for a nucleophilic attack and stabilize the transition state leading to the tetrahedral intermediate. A growing number of organocatalytic systems nicely demonstrate that such hydrogen bond-promoted chemical reactions can be mimicked by well-conceived small molecules that operate in conceptually similar manner (Figure 1).[5−7]

For example, the (thio)urea-based "bidentate" N−H groups (Figure 1) facilitate the addition of CN^- onto ketone/imines.[8,9] Efficient catalytic versions of this and related chemistry have been implemented using a series of crescent-shaped organic structures designed with HBDs, which have significantly advanced our understanding of the structure−reactivity relationships in electrophile activation.[6d,g,i,k] As shown in Figure 1, urea (**I**), thiourea (**II**), and guanidine (**III**) (and its protonated form) all present multiple, polarized N−H groups as effective HBD units. Such structural similarity logically suggests that chemical transformations requiring activation of C═X (X = hydrogen bond acceptor; HBA) group could equally well be effected by C═X···H−N interactions with

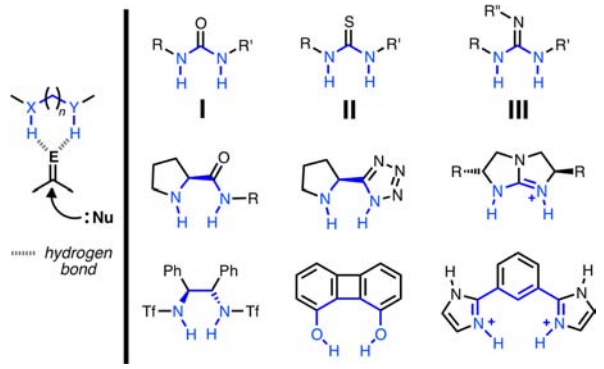

Figure 1. Binding and activation of electrophilic C═E (E = O or NR) group by "double hydrogen bonds" (left) and representative HBD motifs (right), where the functional groups for two-point contacts are highlighted in blue.[5−7]

guanidine-based small molecules. The functional utility of the guanidine motif derives further from the high pK_a value of the guanidinium cation and its ability to participate in strong hydrogen bonds using charged N−H groups. Indeed, structural motifs derived from guanidine and its conjugate acid have recently emerged as potent organocatalysts,[6d,10,11] superbases,[12−14] and electronically/sterically tunable ligands.[15]

A growing number of supramolecular constructs are also found in the literature that exploit guanidine/guanidinium

Received: December 17, 2012
Published: February 6, 2013

functionalities for molecular recognition,[16−19] self-assembly,[20] and switching.[21] Here, the planar {CN_3} core[22] in both neutral and protonated forms allows for facile construction of highly preorganized structures through multiple hydrogen bonds. Moreover, this basic structural motif can be elaborated further by installing a carbonyl group next to the guanidine nitrogen, which enhances both the strength and directionality of the N−H groups. As shown in Figure 2, the intramolecular N−H···O

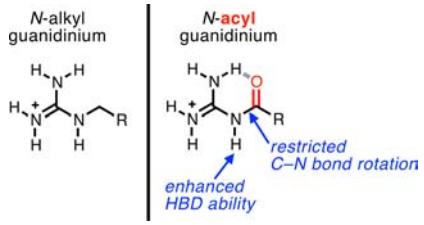

Figure 2. Structural preorganization and enhanced N−H acidity of the guanidinium group with a *N*-acyl substituent.

hydrogen bonding between the guanidine N−H and neighboring carbonyl oxygen atom not only functions as a rigid conformational lock but also enhances the acidity of the N−H proton for strong hydrogen bonds.[23]

In this paper, we disclose the chemistry of a *N*-acylguanidine modified xanthene derivative **1** (Scheme 1) and its application

Scheme 1. Electrophile Activation for Covalent Capture of CN^- Coupled to Fluorescence Turn-On Response

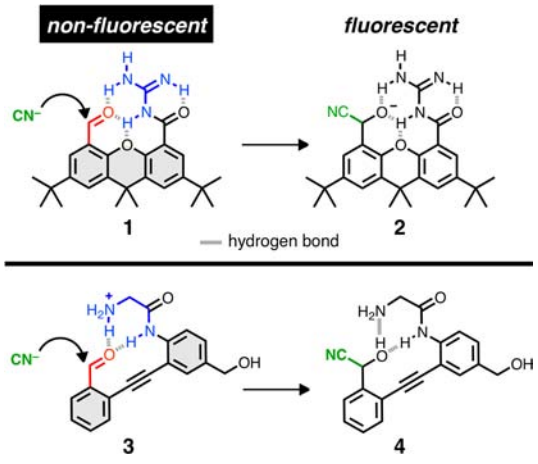

for fluorescence turn-on detection of CN^-. Detailed solution spectroscopic studies on **1** and its structural analogues have unveiled a remarkable strength of the interdigitated hydrogen-bonding network, which allows for a fast and selective capture of cyanide ion to form **2** by activation of the aldehyde C═O group.

Notably, **1** responds rapidly (k = 22.3 M^{-1} s^{-1}) to CN^- by a large (>7-fold) enhancement in the blue emission at λ_{max} = 440 nm. A detailed understanding of the structure−property−reactivity relationship of this cyanide-responsive latent fluorophore was aided by a combination of spectroscopic, X-ray crystallographic, and DFT computational studies. The findings described in this paper contribute to the growing research interests in the use of noncovalent interactions, in particular hydrogen bonds, to direct and facilitate bond-forming chemical reactions of both fundamental and practical importance.

BACKGROUND: DESIGN CONSIDERATIONS

We have previously shown that a bifurcated hydrogen-bonding network can be constructed using a synthetic mimic of peptide β-turn.[24−26] As shown in Scheme 1, multiple intramolecular N−H···O═C contacts in **3**,[26] in its "folded" conformation, effectively polarize the aldehyde C═O group to enhance its reactivity toward CN^- to form the cyanohydrin adduct **4**. This efficient chemical transformation restores the inherent luminescent properties of the diphenylacetylene-based π-conjugation, which enables selective turn-on response toward CN^- under physiologically relevant aqueous conditions.

This initial discovery made with **3** prompted an exploration into new fluorogenic platforms that maintain rapid and selective response toward CN^- through the hydrogen bond-assisted activation of electrophilic site but operate with excitation and emission at longer-wavelength visible region. The latter consideration is to avoid undesired overlaps with background spectral window of biological/environmental samples, which was not fully addressed by **3** requiring photoexcitation at λ_{exc} = 270 nm.

In the quest for a new structural motif that can satisfy both the chemical and photophysical requirements discussed above, we were attracted to the xanthene-based polycyclic systems **IV**−**VII** shown in Figure 3. This particular structural motif has

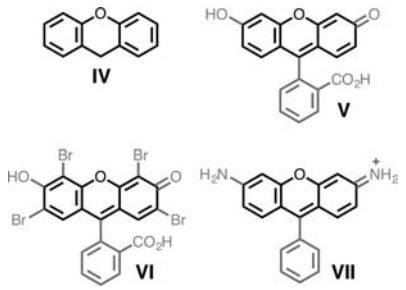

Figure 3. Chemical structures of fluorescein (**V**), eosin (**VI**), and rhodamine (**VII**) as structural derivatives of the parent xanthene system **IV**.

been used extensively as fluorogenic components in molecular probes and imaging agents. As exemplified by fluorescein, eosin, and rhodamine derivatives,[27,28] the practical utility of such system derives from excellent optical properties (i.e., high quantum yields at longer wavelengths) that can readily be modulated either by synthetic modifications or by changes in local environments. While the parent xanthene system has been used extensively as rigid structural scaffolds for shape-persistent oligomer/polymers[29] and multidentate ligands[30,31] as well as templates for molecular recognition and organocatalysis[32] and biomimetic structures,[24c,33] its structural elaboration to fluorogenic cyanide receptor is yet to be demonstrated.

We envisioned that a *N*-acylguanidyl fragment introduced to one side of the xanthene platform should establish multipoint intramolecular HBD−HBA contacts with an aldehyde group installed on the other side of the molecule (Scheme 1). As in the case for **3**, the aldehyde group attached directly to the π-conjugated system of **1** could function as an internal quencher site to promote a rapid intersystem crossing from the [n,π*] singlet state to the [π,π*] triplet state,[34] but its chemical

dx.doi.org/10.1021/ja312313f | J. Am. Chem. Soc. 2013, 135, 3620−3632

transformation to the cyanohydrin adduct **2** could restore the fluorescence. In addition to supporting a rigid π-conjugated skeleton, the oxygen atom at the 9-position of the xanthene ring system participates also in the interdigitated HBD−HBA array (Scheme 1) to enhance the thermodynamic stability of the "folded" conformation (vide infra). Moreover, the *N*-acylguanidyl motif of **1** should further increase the acidity of the N−H proton for a stronger hydrogen bond toward the aldehyde C═O group on the concave side and help rigidify the entire structure through intramolecular N−H···O═C contact on the convex side of the molecule (Scheme 1). A preliminary computational modeling predicted a highly compact structure of **1** without noticeable steric constraints, which convinced us to initiate the synthesis of the actual molecule.

RESULTS AND DISCUSSION

Synthesis. Our synthesis of **1**, as summarized in Scheme 2, commenced with a selective monoesterification of the

Scheme 2. Synthetic Route to 1[a]

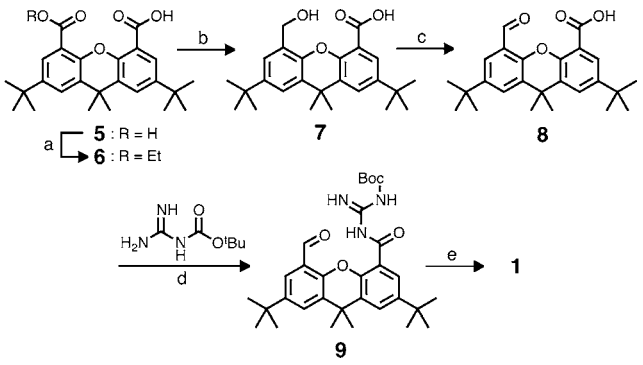

[a](a) DCC, DMAP, EtOH/CH_2Cl_2, 0 °C to rt, 56%. (b) $NaBH_4$, THF/MeOH, 50 °C, >99%. (c) PCC, SiO_2, CH_2Cl_2, rt, 61%. (d) Boc-guanidine, DCC, NMM, HOBt, CH_2Cl_2, rt, 87%. (e) TFA, CH_2Cl_2, reflux, >99%.

dicarboxylic acid **5** to desymmetrize the 1- and 8-positions of the xanthene molecule. Subsequent reduction and oxidation converted **6** to **8** having an aldehyde and a carboxylic acid group facing each other across the xanthene π-platform. A standard amide coupling reaction between **8** and Boc-protected guanidine proceeded cleanly under DCC/HOBt conditions to produce **9**, which was quantitatively converted to **1**, isolated as a white solid after acidic deprotection and basic workup.

Structural Characterization: Interdigitated Hydrogen Bonds. The assembly of the desired hydrogen-bonding network in **1**, as proposed in Scheme 1, was confirmed by crystallographic chemical analysis. Single crystals of **1** suitable for X-ray crystallography were obtained by diffusion of hexamethyl disiloxane into an acetone/CF_3CO_2H solution of the purified material. The compound crystallized as the monoprotonated $[\mathbf{1}\cdot H]^+$ salt with trifluoroacetate as the counteranion (Figure 4).[35]

As shown in Figure 4a, the two N−H groups of the guanidinium fragment in $[\mathbf{1}\cdot H]^+$ point toward the concave side of the molecule and converge at the aldehyde oxygen atom across the "turn" motif with N···$O_{carbonyl}$ distances of 2.759(3) and 2.891(3) Å. In addition, the N1−H group, which is located closest to the xanthene ring, makes another hydrogen-bonding contact (N···O_{ether} = 2.723(3) Å) with the xanthene ether oxygen atom. Such offset "zipper-like" HBD−HBA pattern

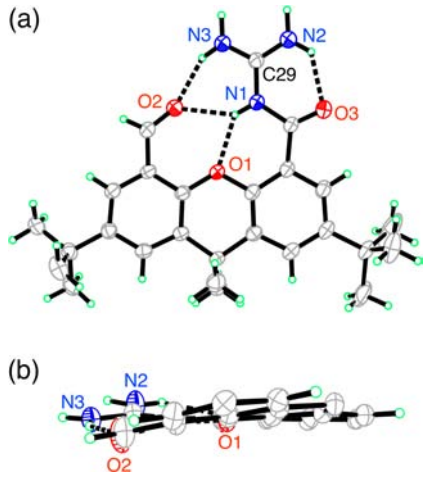

Figure 4. X-ray structure of $[\mathbf{1}\cdot H]^+$ cation as ORTEP diagrams with thermal ellipsoids at 50% probability: (a) face-on and (b) edge-on views. One of the two *tert*-butyl groups on the xanthene ring is disordered over two positions, for which only one model is shown in (a). In (b), the *tert*-butyl and methyl groups have been omitted entirely for clarity. Selected interatomic distances (Å) of the hydrogen bonds that are denoted by dashed lines: N1···O1, 2.723(3); N1···O2, 2.891(3); N3···O2, 2.759(3); N2···O3, 2.614(4).

(with the guanidinyl N−H groups constituting one side of the zipper as HBD; aldehyde and ether oxygen atoms as HBA on the other side of the zipper) maximizes the donor−acceptor complementarity between the HBD and HBA groups without repulsive secondary interactions in the classical Jorgensen model of hydrogen bonds.[36] The conformational stability of $[\mathbf{1}\cdot H]^+$ is enhanced further by the N−H···O hydrogen bond (N···O = 2.614(4) Å) between the guanidinyl N2−H and amide C═O group on the convex side of the molecule. A total of four pairwise HBD−HBA interactions thus contribute collectively to the compact shape (Figure 4a) as well as the essentially coplanar arrangement (Figure 4b) of the molecular skeleton, which is reminiscent of the honeycomb-like lattice with closely packed hexagonal cells for structural strength.

With compelling structural evidence obtained for the interdigitated hydrogen bonds in $[\mathbf{1}\cdot H]^+$, we wished to investigate the presence of similar HBD−HDA arrays in the charge neutral form **1**. As shown in Figure 5a, the energy-minimized DFT model **1′** (without the methyl and *tert*-butyl substituents on the xanthene ring system of **1**) is essentially superimposable onto the computed structure of its mono-protonated form $[\mathbf{1}'\cdot H]^+$. Overall, the conformational stability of the system through interdigitated hydrogen bonds is maintained for both the neutral base **1′** and its conjugate acid $[\mathbf{1}'\cdot H]^+$.

Consistent with the intuitive prediction, a slight contraction of the concave side of the molecule is observed for $[\mathbf{1}'\cdot H]^+$. This minor structural transition arises from the tilting of the guanidinium "arm" unit toward the aldehyde group to make tighter N−H···O contacts, which is the consequence of N−H bond polarization (and therefore stronger hydrogen bond) upon protonation of the guanidinyl group. The metric parameters predicted for the double N−H···O hydrogen bonds between the guanidinyl and carbonyl groups in the DFT model $[\mathbf{1}'\cdot H]^+$ (Figure 5c) are also comparable to the corresponding values of the crystallographically characterized $[\mathbf{1}\cdot H]^+$ (Figure 4).

dx.doi.org/10.1021/ja312313f | J. Am. Chem. Soc. 2013, 135, 3620−3632

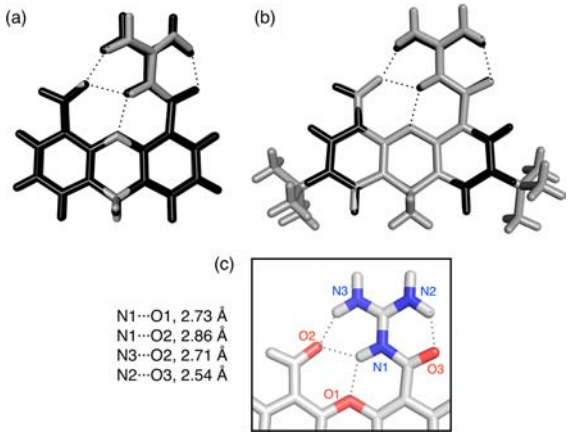

Figure 5. Overlay of the (a) DFT models **1′** (in gray) and $[\mathbf{1}'\cdot H]^+$ (in black) and (b) X-ray structure of $[\mathbf{1}\cdot H]^+$ (in gray) and DFT model $[\mathbf{1}'\cdot H]^+$ (in black) in capped-stick representations with hydrogen bonds denoted by dotted lines. Geometry optimization was performed at the B3LYP/def2-TZVP level of theory with dispersion correction (ORCA 2.9). (c) A close up view of the DFT model $[\mathbf{1}'\cdot H]^+$ and selected interatomic distances, where N is blue and O is red.

Structural Folding in Solution: 1-D and 2-D ^{1}H NMR Spectroscopic Studies. While the X-ray crystallographic and DFT computational studies described in the previous section have suggested the importance of intramolecular hydrogen bonds in the assembly of well-defined secondary structures, the stability of such "folded" conformation in more relevant environment was yet to be established. Toward this objective, we decided to carry out detailed solution ^{1}H NMR spectroscopic studies.

As shown in Figure 6a, the ^{1}H NMR spectrum of **1** in $CDCl_3$ at T = 298 K revealed three sharp N−H resonances. The most downfield shifted signal at δ = 11.5 ppm is associated with the amide N1−H proton of the acylguanidine unit (Figure 6b).[23g,28,37,38] The other two resonances at δ = 10.9 ppm (assigned to N2−H) and 8.9 ppm (assigned to N3−H) are sharp and widely separated, suggesting that the amine/imine units at the guanidinyl end of **1** are in magnetically nonequivalent environment and exchange slowly on the NMR time-scale at rt. The significantly downfield-shifted N−H resonances also implicate the involvement of additional deshielding effects, such as intramolecular hydrogen bonds (Figure 5a).

The long-range $^4J_{H,H}$ scalar coupling (= *w*-coupling) observed in the 2D COSY ^{1}H NMR spectrum (Figure S1) further supports the spectral assignment of these N−H resonances[39] and their spatial relationships predicted by DFT computational studies (Figures 5a and 6b). For example, the N2−H proton shows two independent cross-peaks to N3−H and N1−H resonances, respectively, via *w*-coupling. The relative chemical shifts of these N−H resonances are also in good agreement with the assignments shown in Figure 6.

The precise spatial arrangement of the hydrogen bonding network in **1** was established further by 2D ^{1}H NMR spectroscopy. As shown in Figure 6a, the aldehyde C−H proton of **1** in $CDCl_3$ displays pronounced NOE cross-peaks with both the N1−H and N3−H proton resonances. This spectral pattern is consistent with the DFT geometry optimized model **1′** (Figures 5a and 6b) and establishes that the dual hydrogen bond between the aldehyde C═O and guanidinyl N−H groups is indeed maintained in solution.

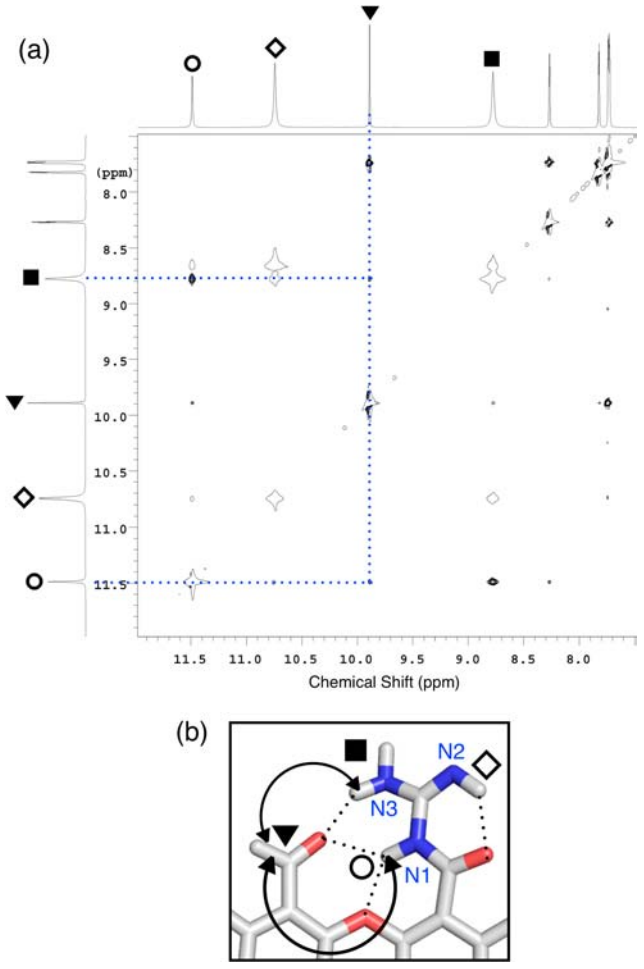

Figure 6. (a) Partial 2D-NOESY contour plot of **1** (= 100 mM) in $CDCl_3$ at T = 298 K. The corresponding 1D spectrum is shown along the ordinate. The symbols ○, ◇, ■, and ▼ denote the resonances of the N1−H, N2−H, N3−H, and aldehyde C−H proton, respectively. (b) Capped-stick representation of the DFT geometry optimized model **1′** (Figure 5a) in a close-up view, with hydrogen bonds (in dotted lines) and NOE contacts (in double-headed arrows) denoted and the protons labeled with the same symbols as in (a).

We note that the N3−H and N2−H proton resonances appear as similar intensities (Figure 6a), whereas the chemical structure of **1** would predict a 2:1 peak integration ratio. This spectral behavior suggests a rapid tautomerization involving proton exchange between N2 and N3. Among the four protons of **1** that are associated with the three guanidyl nitrogen atoms N1, N2, and N3, three protons tightly engage in hydrogen bonds (Figure 6b) and are therefore less mobile. The remaining fourth proton, however, can exchange between the N2 and N3 positions at the guanidinyl end. The distinctively different chemical (and therefore magnetic) environments of the N2−H and N3−H protons still give rise to well-resolved ^{1}H NMR resonances (Figure 6a), but the ΔpK_a values between the two conjugate acids must be sufficiently small to establish resonance-assisted tautomeric equilibrium by fast proton exchange,[40] which was observed experimentally.

How Strong is the Interdigitated Hydrogen Bond? One important principle behind the design of **1** is structural preorganization through a contiguous array of HBD−HBA. As shown in Schemes 1 and 2, both **1** and its synthetic precursor **9** share an essentially identical π-conjugated backbone but differ

dx.doi.org/10.1021/ja312313f | J. Am. Chem. Soc. 2013, 135, 3620−3632

in the guanidinyl *N*-substituent. The presence of the bulky *N*-Boc group in **9** was anticipated not only to increases the steric crowding but also to decrease the strength of the N−H···O═C hydrogen bond across the turn motif, compared to **1** having the unsubstituted N−H terminal group. Through hydrogen bonds, the electronic properties of the aldehyde group should respond sensitively to such structural modification in the "remote" site. In order to test this postulation, a direct NMR spectroscopic comparison was made between **1** and **9**.

In $CDCl_3$, the ^{13}C NMR spectra of **1** and **9** showed only a subtle change in the chemical shifts of the aldehyde carbon atoms and were thus less informative (see Experimental Section). In contrast, the aldehyde C−H proton resonance of the Boc-substituted **9** (Figure 7a) is significantly ($\Delta\delta$ = 0.77 ppm) downfield-shifted relative to that of **1** (Figure 7b). Such spectral difference could be rationalized by an increased deshielding from the weakly hydrogen-bonded C═O π-system of **9** relative to **1**.[41] The reduced conformational rigidity of **9** also allows its N−H protons to undergo rapid exchange to produce very broadened ^1H NMR spectral features (Figure 7a). In stark contrast, **1** displays sharp and well-resolved N−H resonances under similar conditions (Figures 6 and 7b), reflecting their association with tighter hydrogen bonds and therefore slower exchange.

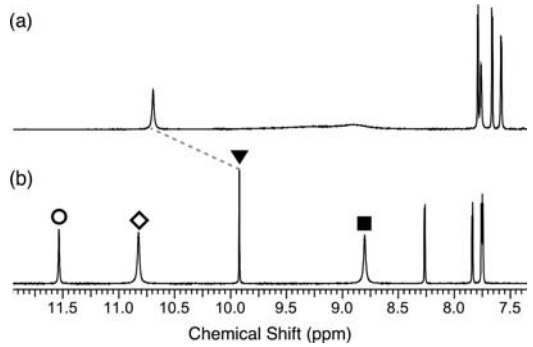

Figure 7. Partial ^1H NMR spectra of (a) **9** and (b) **1** (30.0 mM) in $CDCl_3$, at T = 298 K, with the aldehyde C−H resonances indicated by dashed lines. The sharp N−H peaks of **1** (see Figure 6 for the labeling schemes) become indistinguishably broadened for the Boc-substituted **9**.

The strength of the intramolecular hydrogen bonds in **1** was examined further by concentration-dependent ^1H NMR studies. Within the concentration range of [**1**] = 2.0−100 mM in $CDCl_3$ at T = 298 K (Figure S2), no detectable shift in resonance was observed for the amide N1−H and guanidinyl N3−H protons, which engage in double hydrogen bonds with the aldehyde group (Figure 6). In contrast, the sterically less protected N2−H group located on the convex side of the molecule undergoes a slight upfield shift at higher concentrations. Over a wide range of concentrations, **1** retains its compact folded conformation through tight intramolecular hydrogen bonds, despite that intermolecular interactions would compete more effectively with increasing concentration.

Strength of Hydrogen Bond Determined by the Energetics of Bond Rotation. The conformational stability of **1**, described in the previous section, is tied closely to the restricted bond-rotating motions of the guanidinyl unit. A quantitative understanding of this process, as shown in Scheme 3, was aided by variable-temperature (VT) ^1H NMR spectroscopic studies.

Scheme 3. Exchange of Hydrogen-Bonded N−H Protons through Terminal C−N Bond Rotation

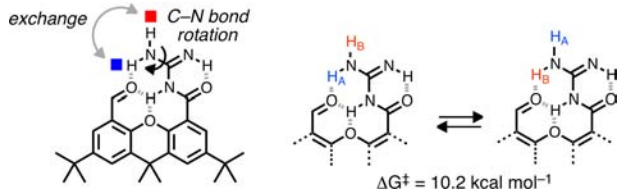

As shown in Figure 8, the two N3−H protons on the guanidinyl group of **1** (labeled as H_A and H_B in Scheme 3) appear as a singlet at δ = 8.80 ppm in $CDCl_3$ at T = 298 K. Upon lowering the temperature, however, this signal broadens and eventually splits into two resonances at δ = 9.38 and 8.43 ppm at T = 223 K, reflecting a restricted rotation about the C−N bond shown in Scheme 3.[42] Within this temperature range, the N1−H proton resonance at δ = 11.46 ppm and the N2−H signal at δ = 10.98 ppm remain largely unchanged and appear as sharp singlets, which is consistent with their participation in stronger hydrogen bonds (vide infra).

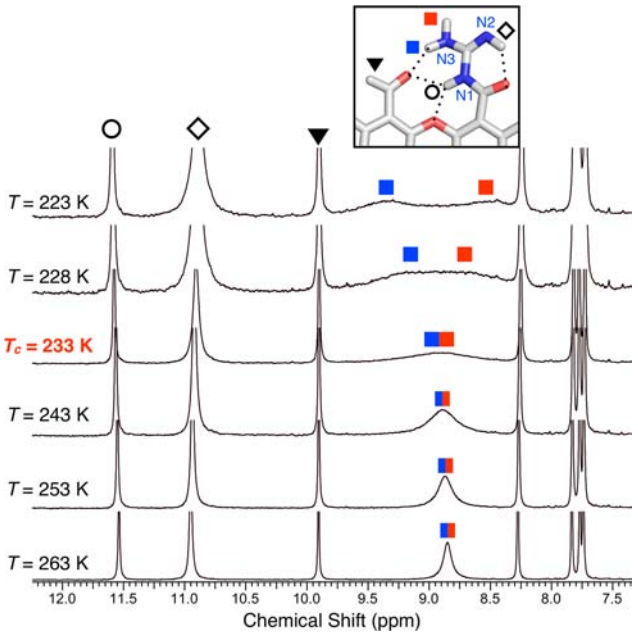

Figure 8. Partial ^1H NMR spectra of **1** (30.0 mM) in $CDCl_3$ obtained at various temperatures (T = 223−263 K) and referenced to the proton labeling scheme shown next to the top spectrum.

Using the $\Delta\nu$ value (= 381 Hz) at the slow exchange limit and the coalescence temperature (T_c = 233 K) (eqs 1 and 2), the energy barrier of $\Delta G^{\ddagger}$ = 10.2 kcal mol^{-1} was determined for the C−N rotation depicted in Scheme 3.[43]

$$k_c = \frac{\pi}{\sqrt{2}}|\Delta\nu| \quad (1)$$

$$\Delta G^{\ddagger} = RT_c \ln\left(\frac{RT_c}{k_c N_A h}\right) \quad (2)$$

Unlike the N1−H proton, which is buried deeply inside the concave side, the N2−H and N3−H groups on the guanidinyl end of the molecule reside on the convex surface of the molecule (Figures 5 and 6b) and therefore respond more

dx.doi.org/10.1021/ja312313f | J. Am. Chem. Soc. 2013, 135, 3620−3632

sensitively to changes in the solvent environment. Indeed, upon changing the solvent from $CDCl_3$ to CD_3CN, the N2−H resonance of **1** undergoes a significant ($\Delta\delta$ = 1.49 ppm) upfield shift, whereas the rest of the spectral pattern remains largely unchanged (compare Figures 8 and 9).

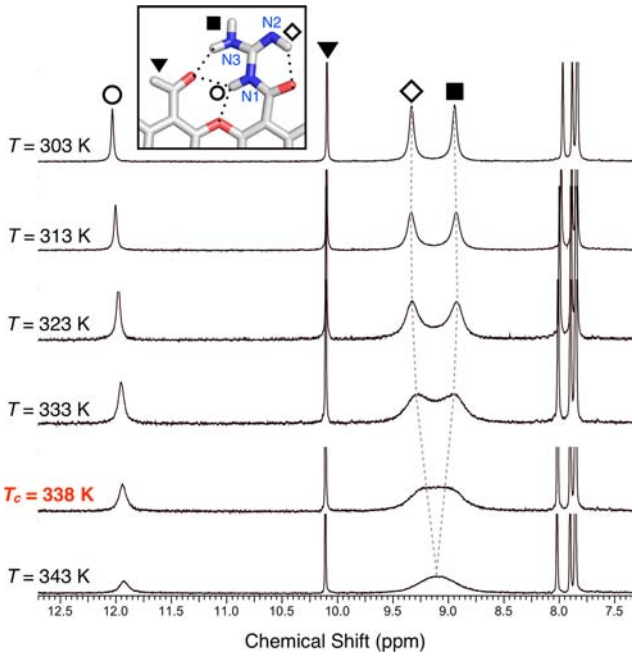

Figure 9. Partial ^{1}H NMR spectra of **1** (30.0 mM) in CD_3CN obtained at various temperatures (T = 303−343 K) and referenced to the proton labeling scheme shown next to the top spectrum.

This spectral behavior implicates weakening of the N−H···O=C_{amide} contact in more polar solvent environment (E_T(30) = 39.1, $CHCl_3$; 46.7, CH_3CN).[44] At T = 303 K, the N2−H and N3−H protons appear as two well-resolved signals at δ = 9.33 and 8.94 ppm, respectively, but broaden with increasing temperature and eventually coalesce at T = 338 K (Figure 9). Such temperature-dependent spectral change could best be explained by the rotation about the guanidinyl C−N bond (Scheme 4) which exchanges the N2−H and N3−H sites.

Scheme 4. Exchange of Hydrogen-Bonded N−H Protons through Internal C−N Bond Rotation

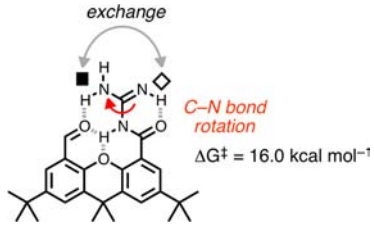

The VT ^{1}H NMR data shown in Figure 9 (T_c = 338 K; $\Delta\nu$ = 151 Hz) was thus analyzed using eqs 1 and 2 to derive the rotational energy barrier of $\Delta G^{\ddagger}$ = 16.0 kcal mol^{-1} for the "internal" C−N bond (Scheme 4). Even with assistance from the more polar solvent environment (vide supra), this value is significantly higher than that ($\Delta G^{\ddagger}$ = 10.2 kcal mol^{-1}) of the "terminal" (and therefore less restricted) C−N bond rotation (Scheme 3). The chemical structure of **1** dictates that the C−N bond rotation shown in Scheme 4 should require concerted (if not synchronous) breaking of at least two N−H···O hydrogen bonds. As such, this process has a higher energy barrier ($\Delta\Delta G^{\ddagger}$ = 5.8 kcal mol^{-1}) than the terminal C−N bond rotation (Scheme 3) which requires disruption of only one N−H···O contact. Our VT NMR studies have thus provided quantitative experimental support for this chemically intuitive structure−dynamics model.

In summary, the honeycomb-shaped multiple HBD−HBA contacts in **1** serve as a robust conformational lock to suppress internal rotational motions and create distinctively different chemical environments around the guanidinyl HBD unit. The solvent- and temperature-dependent dynamic behavior of these N−H groups has provided unique opportunities to use VT ^{1}H NMR spectroscopy to quantify directly the strength of intramolecular hydrogen bonds as reflected on the differential activation energies ($\Delta\Delta G^{\ddagger}$) of the C−N bond rotation. Notably, the high-energy barrier ($\Delta G^{\ddagger}$ = 16.0 kcal mol^{-1}) for the bond twisting around the internal C−N bond (Scheme 4) ensures that the two N−H groups are properly directed toward the CHO group for a tight two-point contact (Figures 5 and 6).

Covalent Capture of Cyanide Ion and Turn-On Fluorescence Response. In addition to restricting internal torsional motions to increase the conformational stability, the intramolecular hydrogen bonds in **1** should further polarize the C=O group to promote its reactivity toward nucleophilic attack (Scheme 1). This hypothesis was investigated by the reaction between **1** and CN^-.

As shown in Figure 10a, addition of CN^- (100 equiv; delivered as NaCN salt) to a solution of **1** (30 μM) in buffered

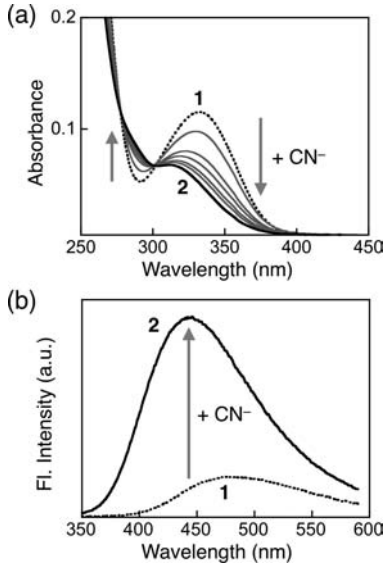

Figure 10. (a) Time-dependent (0−30 s) changes in the UV−vis spectra of **1** (= 30 μM) treated with NaCN (100 equiv) and (b) fluorescence spectra of **1** (= 10 μM) prior to (dotted lines) and after (solid lines) addition of NaCN (300 equiv) in H_2O:CH_3CN = 9:1 (v/v) at pH = 7.0 (HEPES, 100 mM).

(pH = 7.0; HEPES, 100 mM) H_2O−CH_3CN (9:1, v/v) resulted in a decrease in the electronic absorption at λ_{max} = 320 nm with concomitant buildup of a new band at λ_{max} = 290 nm. The presence of the isosbestic points at λ = 280 and 300 nm indicated a clean conversion of the reactant to the product with

dx.doi.org/10.1021/ja312313f | J. Am. Chem. Soc. 2013, 135, 3620−3632

no build-up of spectroscopically detectable intermediates or byproducts.

Under similar conditions, **1** displays a weak (Φ_F = 2.4%) fluorescence at $\lambda_{max,em}$ = 480 nm upon excitation at λ_{exc} = 300 nm. The addition of CN^- (300 equiv; delivered as NaCN salt), however, immediately elicited a large (>7-fold) enhancement in the emission intensity (Φ_F = 17.2%) (Figure 10b). Notably, the fluorescence turn-on response from the reaction product occurred at $\lambda_{max,em}$ = 440 nm, which is significantly red-shifted than that ($\lambda_{max,em}$ = 370 nm) of the first-generation β-turn mimic **4** (Scheme 1).

The chemical structure of the reaction product was established by a combination of $^1H/^{13}C$ NMR spectroscopy and high-resolution mass spectrometry. As shown in Figure 11,

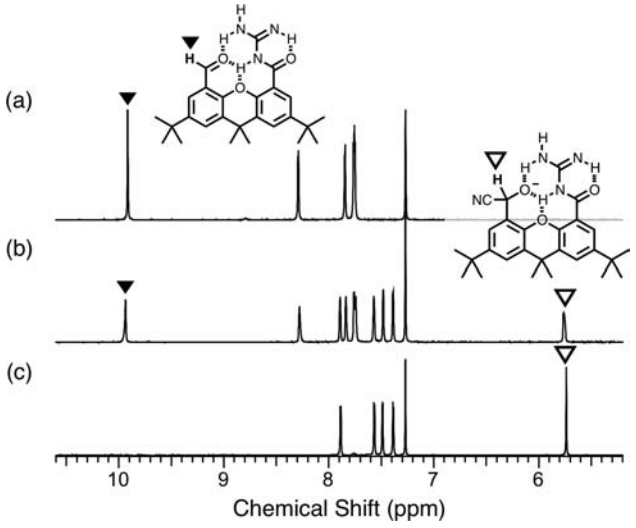

Figure 11. Partial ^1H NMR spectra of (a) **1** (= 30 mM) and **1** + CN^- (3.0 equiv) obtained (b) 1 min and (c) 10 min after addition of NaCN in $CDCl_3$ mixed with 2.5% (v/v) of D_2O at T = 298 K. The proton resonances of benzaldehyde C−H group in **1** (▼) and the benzyl alcohol C−H group in **2** (▽) are labeled using the symbols denoted in the corresponding chemical structure; the N−H proton resonances disappeared as a result of H/D exchange with D_2O.

the reaction between **1** (30 mM) and NaCN (3 equiv) in $CDCl_3$ (doped with D_2O, 2.5%, v/v) was completed within 10 min, as evidenced by the disappearance of the aldehyde C−H resonance at δ = 9.91 ppm of **1** and the growth of the benzylic C−H resonance at δ = 5.74 ppm from the cyanohydrin adduct **2** (Scheme 1). The aromatic resonances also showed systematic upfield shifts upon **1**-to-**2** conversion.

This spectral assignment was further corroborated by ^{13}C NMR spectroscopic studies on the reaction mixture (Figure S3), which revealed the appearance of two new resonances from the benzylic (δ = 60.8 ppm) and cyanyl (δ = 117.6 ppm) carbons, with the loss of the aldehyde (δ = 194.0 ppm) signal. High-resolution ESI-MS analysis also identified a peak for the cyanohydrin adduct **2**: calcd for $C_{27}H_{35}N_4O_3$ $[M + H]^+$, 463.2709; found, 463.2697 (Figure S4).

Kinetic Studies: Structure−Reactivity Relationships. The underlying molecular mechanism of the turn-on fluorescence response of **1** toward CN^- (Figure 10b) involves an efficient chemical transformation of the aldehyde group, functioning as the fluorescence quencher group[34] as well as the cyanide receptor site,[26] and subsequent restoration of the xanthene fluorescence. As shown in Figure 12, the homologous

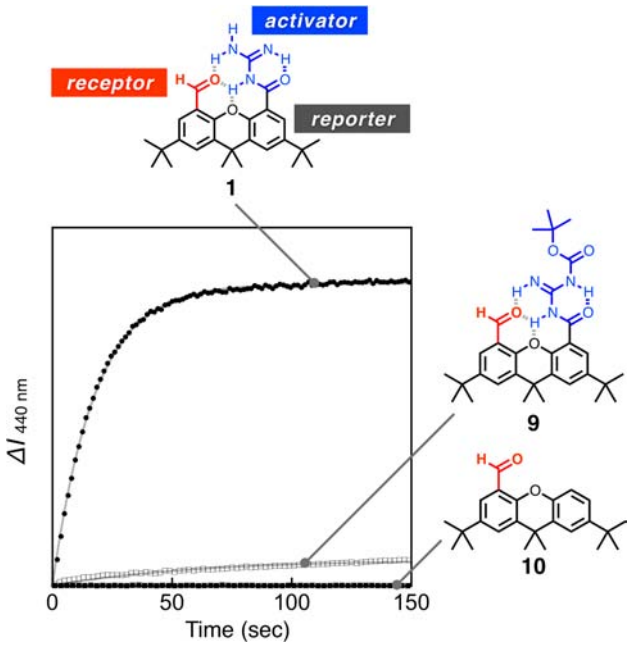

Figure 12. Time-dependent changes in the fluorescence intensity at λ_{em} = 440 nm (λ_{exc} = 300 nm) observed in the reactions of **1** (●), **9** (□), and **10** (■) with NaCN (2.50 mM) in H_2O:CH_3CN = 2:1 (v/v) (pH = 7.0; HEPES, 100 mM) at T = 298 K; sample concentration =10.0 μM. The gray curves overlaid on the experimental data points of **1** and **9** are theoretical fits generated using k' = 5.6 × 10^{-2} s^{-1} for **1** and k' = 9.4 × 10^{-4} s^{-1} for **9** (eq 3). No change in the fluorescence intensity was observed for **10** under this condition.

set of molecules **1**, **9** and **10** commonly share these key structural/functional components (i.e., quencher/receptor site juxtaposed to the fluorogenic reporter) and therefore should react similarly toward CN^-. The efficiency of this chemical transformation, however, would depend critically on the strength of the N−H···O═C hydrogen bonds to activate the electrophilic carbonyl group.

An experimental validation for this structure−reactivity model was aided by comparative kinetic studies on **1**, **9**, and **10** (Figure 12). Due to the limited water solubility of **9** and **10**, reactions were carried out in H_2O−CH_3CN (2:1, v/v) mixed solvent system at pH = 7.0 (HEPES, 100 mM) and monitored with the fluorescence intensity at λ = 440 nm as a function of time. Under *pseudo*-first-order conditions, an exponential growth in the emission intensity was observed for the reaction between **1** and CN^- at T = 298 K (Figure 12). A linear dependence of the *pseudo*-first-order rate constant k' (= $k[CN^-]_0$; eq 3) on $[CN^-]_0$ (Figure S5) suggests a rate-determining C−C bond formation by bimolecular addition reaction:

$$\frac{\Delta I}{I} = 1 - e^{-k't} \quad (3)$$

Apparently, the stronger N−H···O═C hydrogen bonds in the conformationally better defined **1** lead to a remarkable (> 60-fold) enhancement in the reactivity, as reflected on the second-order rate constant of k = 22.3 M^{-1} s^{-1} of **1** vs k = 0.37 M^{-1} s^{-1} of **9** at T = 298 K (Figure S5). Changes in the ionic strength (by adding NaCl up to 0.2 M) did not affect either the response rate of **1** or the fluorescence intensity of its cyanohydrin adduct (Figure S6). Under similar conditions, **10**

dx.doi.org/10.1021/ja312313f | J. Am. Chem. Soc. 2013, 135, 3620−3632

lacking any hydrogen bonds shows no reactivity toward CN^- (Figure 12).

Electrophile Activation through Hydrogen Bonds: Quantifying the Electronic Basis of Chemical Reactivity. An intuitive chemical model to rationalize the differential reactivity observed along the series **1** > **9** ≫ **10** (Figure 12) is the activation of electrophilic C═O group through intramolecular hydrogen bonds (Scheme 1). In order to obtain a more quantitative measure of this process that is fundamentally rooted in the electronic structures, we have investigated **1′**, $[\mathbf{1'}\cdot H]^+$, and **10′** (Figure 13), as simplified DFT computational models of the corresponding molecular system **1**, $[\mathbf{1}\cdot H]^+$, and **10**, respectively.

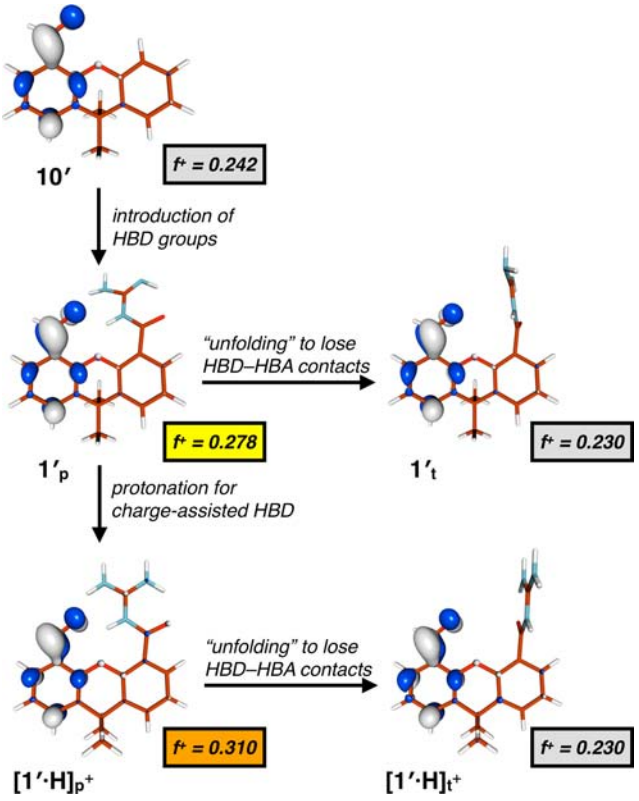

Figure 13. Electrophilic FMOs of the DFT models **1′**, $[\mathbf{1}\cdot H]^+$, and **10′** and the corresponding atomic Fukui index (f^+) of the carbon atom of the aldehyde group functioning as the cyanide capturing site.

Here, an increasing number of N–H HBD groups (e.g., **10′** vs **1′**), including charge-assisted interactions (e.g., **1′** vs $[\mathbf{1'}\cdot H]^+$), were introduced to converge at the C═O group across the "turn" motif defined by the xanthene skeleton. For **1′** and $[\mathbf{1'}\cdot H]^+$, the two distinctively different rotamers, i.e., one with hydrogen bonds (such as $\mathbf{1'}_p$; "planar") and the other without hydrogen bonds (such as $\mathbf{1'}_t$; "twisted"), were considered in order to better quantify the conformational, rather than simple substitution effects of the HBD groups on the C═O bond activation. Since **10′** does not have such HBD groups, only the energetically most favored, planar conformation was studied (Figure 13).

As shown in Scheme 1, the carbon atom of the aldehyde carbonyl group is the reactive site for the covalent capture of CN^-. Therefore, the contribution of the atomic orbital of this carbon atom to the LUMO could be used as a reasonable first-principle descriptor for the chemical reactivity toward nucleophiles. In order for such analysis to be meaningful, the transition state leading to the product should lie closer to the reactants, rather than the products side. In addition, the reaction should be closer to the idealized soft–soft interaction, rather than the hard–hard extreme, since electrostatic factors are not adequately described by Fukui reactivity index.[45,46] Fortuitously, the covalent capture of cyanide anion by a carbonyl group, shown in Scheme 1, satisfies these two important requirements.[47]

For the DFT models shown in Figure 13, we have determined their atomic Fukui functions from atomic Mulliken population of the electrophilic FMOs. While the absolute magnitude of this parameter f^+ might have limited practical use, comparisons made across intimately related structural homologues, such as **1′**, $[\mathbf{1'}\cdot H]^+$, and **10′**, in which the electrophilicity of the C═O carbon center is varied systematically by its immediate chemical environment, should provide important and quantifiable insights into the structure–reactivity relationship (Figure 12).

Consistent with our intuitive prediction, the LUMO of each system shown in Figure 13 is localized at the aldehyde π^* MO[48] and comparable f^+ parameters (0.230–0.242) were obtained for **10**, $\mathbf{1'}_t$, and $[\mathbf{1'}\cdot H]^+_t$. Upon structural "folding" to allow the guanidinyl group to engage in HBD–HBA contacts, however, the f^+ value is significantly increased to +0.278 (for $\mathbf{1'}_p$). Moreover, protonation of this guanidinyl group led to a further increase in the degree of C═O bond polarization, as reflected on the f^+ value of +0.310 computed for $[\mathbf{1'}\cdot H]^+_p$, which is the highest among the series sampled (Figure 13).

The pK_a value of 7.20 (±0.03) determined for **1** (Figure S7) suggests that this molecule should coexist with its conjugate acid $[\mathbf{1}\cdot H]^+$ (Figure 4) in neutral aqueous solutions. As predicted in Figure 13, the guanidinium group of the $[\mathbf{1}\cdot H]^+$ cation should further enhance the reactivity of the aldehyde group through charge-assisted hydrogen bond.[49] Such interaction is not allowed for the Boc-protected **9**, which shows significantly lower response kinetics (Figure 12). We thus conclude that the combination of enhanced conformational rigidity rendered by tighter HBD–HBA contacts (Figures 4–6) and stronger polarization of the C═O group (Figure 13) are responsible for the efficient conversion of **1** to **2** upon reaction with CN^- (Scheme 1).

Selectivity in Cyanide Response. The fluorescence turn-on detection of cyanide by **1** (Figure 10b) relies critically on the clean (Figure 11) and fast C–C bond forming reaction under ambient conditions (Figure 12). Among 15 different anions screened under identical conditions, including F^-, Cl^-, Br^-, I^-, N_3^-, SCN^-, AcO^-, NO_3^-, ClO_4^-, PF_6^-, HCO_3^-, HSO_4^-, $H_2PO_4^-$, and OH^-, the fluorescence turn-on response of **1** works exclusively for CN^- at pH = 7 (Figures 14a,c), with good linearity between the emission intensity and concentration observed down to $[CN^-]$ = 10 μM (Figure S8) and consistent fluorescence enhancement at pH = 6–11 (Figure S9). As shown in Figure 14d, a consistent enhancement in the fluorescence intensity was also observed in competition studies when CN^- was subsequently added to the solutions containing other anions. The high selectivity of **1** in cyanide detection was demonstrated further in extreme competition. For this purpose, a solution of **1** was treated with all 14 different anions combined, which showed only weak background signal. Upon addition of cyanide to this mixture, an immediate enhancement in fluorescence was observed (Figure 14b).

dx.doi.org/10.1021/ja312313f | J. Am. Chem. Soc. 2013, 135, 3620–3632

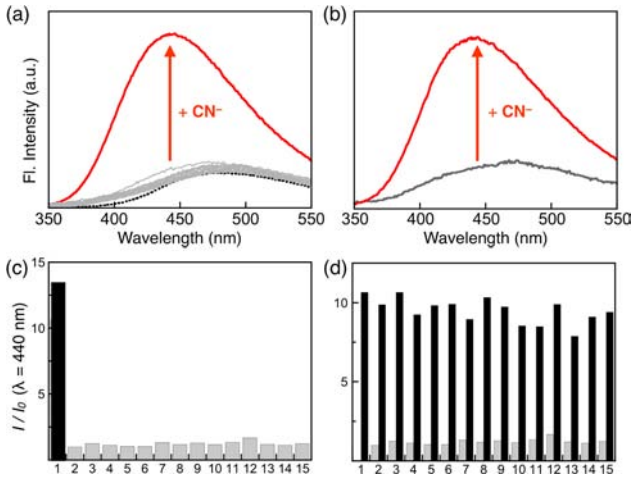

Figure 14. (a) Fluorescence spectra of **1** after exposure to CN^- (in red) or other 14 anions (in gray; see the list in (c) and (d)). For the sample (b), CN^- was added to a solution of **1** + all 14 anions combined. (c) Relative fluorescence response of **1** to various anions. The signal intensity (= I) at λ = 440 nm after treatment of **1** with each anion is normalized with that of **1**-only (= I_0). The bars represent the normalized emission (= I/I_0) of **1** in the presence of the anions of interest: 1, CN^-; 2, F^-; 3, Cl^-; 4, Br^-; 5, I^-; 6, N_3^-; 7, SCN^-; 8, AcO^-; 9, NO_3^-; 10, ClO_4^-; 11, PF_6^-; 12, HCO_3^-; 13, HSO_4^-; 14, $H_2PO_4^-$; 15, OH^-, all delivered as sodium salts. (d) The selectivity of **1** for CN^- in the presence of various anions. The light-gray bars represent the emission of **1** in the presence of 300 equiv of the anion of interest. The black bars indicate the change in the emission that occurs upon subsequent addition of 300 equiv of CN^- to the solution containing **1** and the anion of interest. Conditions: λ_{exc} = 300 nm; T = 298 K; [**1**] = 10.0 μM in H_2O:CH_3CN = 9:1 (v/v) at pH = 7.0 (HEPES, 100 mM).

SUMMARY AND OUTLOOK

As a rigid π-conjugated structural platform, 1,8-disubstituted xanthene can support multiple, honeycomb-shaped HBD–HBA contacts across the turn motif. Taking advantage of this structural feature, we have constructed a cyanide-responsive latent fluorophore **1**, in which an interdigitated array of intramolecular hydrogen bonds function as a "remote activator" for the electrophilic carbonyl group. A facile C–C bond-forming reaction with CN^- redirects the de-excitation pathways of the adduct **2** to elicit a large enhancement in the emission intensity. Using comparative spectroscopic, kinetic, and DFT computational studies, we have investigated the functional role of the hydrogen bonds in conformational preorganization, the molecular mechanism of electrophile activation, and the underlying structure–reactivity relationships dictated by FMO electronic structures.

Prevailing design strategies for cyanide-responsive small-molecules exploit CN^- functioning as a Lewis basic ligand or as a nucleophilic agent. For example, luminescent receptors have been built with Lewis acidic boron centers[50,51] or transition-metal ions,[52] but fluorescence quenching upon CN^- binding (= "turn-off" response) is less desirable.[50c,51a,b] Alternatively, weakly bound and fluorescence-quenching transition-metal ions can be sequestered by coordination to CN^-, and the fluorogenic free ligands thus released can give rise to a net enhancement in luminescence intensity.[53,54]

Upon reaction with CN^- functioning as a nucleophile, the light-absorbing[55] or light-emitting properties[56] of certain chromophore/fluorophores can be changed dramatically. The C–C bond formation required for such reaction-based fluorescence turn-on detection scheme[57] has been implemented with (i) ring-opening reactions of coumarin-fused spiropyrans,[56a,b] (ii) benzyl rearrangement,[56c] and (iii) Michael addition to α,β-unsaturated ketone or dicyano vinyl[56d–i] as well as (iv) addition to π-conjugated carbonyl group (as the most well-explored design strategy).[26,56j–r] In such chemical transformations, the electrophilicity of the reactive sp^2-carbon atom can further be enhanced by (i) installation of positively charged heteroatom substituent,[56s–v] (ii) attachment to electron-withdrawing group (such as CF_3),[56j,k,p,q] and/or (iii) tight association with intramolecular hydrogen bonds.[26,56d,j–r]

Unlike conceptually related systems in which only a single N–H···O=C or O–H···O=C contact can be installed for electrophile activation,[56d,j–r] our structure design allows for the installation of multiple, charge-assisted hydrogen bonds that dramatically accelerate the cyanide-capturing event under ambient conditions but without compromising the selectivity. Efforts are currently underway in our laboratory to expand the scope of the chemistry and find practical applications in device settings.

EXPERIMENTAL SECTION

General Considerations. All reagents were obtained from commercial suppliers and used as received unless otherwise noted. The solvents THF and dichloromethane were saturated with nitrogen and purified by passage through activated Al_2O_3 columns under nitrogen (Innovative Technology SPS 400). Aqueous solutions for reactivity studies and kinetic studies were prepared using H_2O purified by an E-pure water filtration system (Barnstead Thermolyne Co.). The compounds 2,7-di-*tert*-butyl-9,9-dimethyl-xanthene-4,5-dicarboxylic acid (**5**)[32a] and 2,7-di-*tert*-butyl-9,9-dimethyl-xanthene-4-carbaldehyde (**10**)[58] were prepared according to literature procedures. All air-sensitive manipulations were carried out under nitrogen atmosphere by standard Schlenk-line techniques.

Physical Measurements. ^1H NMR and ^{13}C NMR spectra were recorded on a 400 MHz Varian Inova NMR Spectrometer. Chemical shifts were reported versus tetramethylsilane and referenced to the residual solvent peaks. High-resolution chemical ionization (CI) (using CH_4 as CI reagent) and electrospray ionization (ESI) mass spectra were obtained on a Thermo Electron Corporation MAT 95XP-Trap. High-resolution GC-MS (CI, using CH_4 as CI reagent) was obtained on a Thermo Electron Corporation MAT 95XP-Trap. FT-IR spectra were recorded on a Nicolet Avatar 360 FT-IR spectrometer with EZ OMNIC E.S.P. software. UV–vis spectra were recorded on an Agilent 8453 UV–Visible spectrophotometer with ChemStation. Fluorescence spectra were recorded on a Photon Technology International QM-4-CW Spectrofluorometer with FeliX32 software.

Kinetic Studies. The comparative kinetic studies on **1**, **9**, and **10** were conducted in a mixed solvent system of H_2O:CH_3CN = 2:1 (v/v) (pH = 7.0, HEPES 100 mM) due to the limited water solubility of **9** and **10**. Time-dependent changes in the fluorescence intensity were monitored at λ = 440 nm (λ_{exc} = 300 nm) at T = 298 K with constant stirring. The ΔI vs t kinetic traces were fitted by nonlinear regression methods (OriginPro 8.6) using eq 3, in which the parameters k' (= $k[CN^-]_0$) and I (= intensity at $t \rightarrow \infty$) were allowed to vary.

*2,7-Di-tert-butyl-5-formyl-9,9-dimethyl-N-(N-tert-butoxycarbonyl)carbamimidoyl)-xanthene-4-carboxamide (**9**).* To a stirred CH_2Cl_2 (20 mL) solution of **8** (0.291 g, 0.738 mmol), *N*,*N*′-dicyclohexylcarbodiimide (0.239 g, 1.16 mmol), and hydroxybezotriazole (0.159 g, 1.17 mmol) was added Boc-guanidine (0.235 g, 1.48 mmol). A portion of *N*-methylmorpholine (0.15 mL, 1.364 mmol) was added in dropwise fashion, and the mixture was stirred for 5 h. The reaction was quenched by treating with H_2O (10 mL). The organic fraction was extracted with CH_2Cl_2, dried over anhyd $MgSO_4$, and filtered. Volatile fractions were removed under reduced pressure, and the residual material was purified by flash column chromatography on

dx.doi.org/10.1021/ja312313f | J. Am. Chem. Soc. 2013, 135, 3620–3632

SiO_2 (hexane:EtOAc = 5:1, v/v) to furnish **9** as a white solid (0.344 g, yield = 87%). ^{1}H NMR (400 MHz, $CDCl_3$, 298 K): δ 10.69, 7.80−7.81 (d, J = 2.3 Hz, 1H), 7.75 (s, 1H), 7.67−7.68 (d, J = 2.3 Hz, 1H), 7.58−7.59 (d, J = 1.9 Hz, 1H), 1.67 (s, 6H), 1.41 (s, 9H), 1.34 (s, 9H), 1.33 (s, 9H). ^{13}C NMR (100 MHz, $CDCl_3$, 298 K): δ 190.2, 159.1, 150.4, 146.5, 146.4, 146.2, 130.8, 129.1, 126.5, 126.1, 123.6, 123.1, 81.1, 77.4, 36.8, 34.8, 34.7, 32.1, 31.6, 31.5, 31.4, 28.1. FT-IR (thin film on NaCl, cm^{-1}): 3400, 3054, 2987, 2686, 2520, 2410, 1631, 1422, 1264, 1152, 909, 739. HRMS (ESI) calcd for $C_{31}H_{42}N_3O_5$ $[M + H]^+$, 536.3124; found, 536.3146.

*2,7-Di-tert-butyl-N-carbamimidoyl-5-formyl-9,9-dimethyl-xanthene-4-carboxamide (**1**).* A stirred CH_2Cl_2 (10 mL) solution of **9** (0.337 g, 0.628 mmol) and trifluoroacetic acid (10 mL) was heated at reflux overnight. The reaction was cooled to rt and quenched by treating with saturated aq solution of $NaHCO_3$. The organic fraction was extracted with CH_2Cl_2, dried over anhyd $MgSO_4$, and filtered. Volatile fractions were removed under reduced pressure, and the residual material was purified by flash column chromatography on SiO_2 (CH_2Cl_2:MeOH = 10:1, v/v) to furnish **1** as a white solid (0.274 g, yield = 99%). ^{1}H NMR (400 MHz, $CDCl_3$, 298 K): δ 11.54 (s, 1H), 10.82 (br s, 2H), 9.92 (s, 1H), 8.80 (br s, 2H), 8.26−8.27 (d, J = 2.7 Hz, 1H), 7.83−7.84 (d, J = 2.3 Hz, 1H), 7.74−7.76 (m, 2H), 1.71 (s, 6H), 1.41 (s, 9H), 1.37 (s, 9H). ^{13}C NMR (100 MHz, $CDCl_3$, 298 K): δ 194.0, 166.1, 157.2, 148.1, 147.7, 146.4, 146.1, 133.3, 131.7, 131.0, 130.2, 129.9, 129.5, 122.4, 117.6, 34.9, 34.8, 34.3, 33.3, 31.3. FT-IR (thin film on NaCl, cm^{-1}): 3380, 3237, 3055, 2969, 2868, 2681, 1710, 1692, 1612, 1444, 1396, 1265, 1187, 1137, 896, 737. HRMS (ESI) calcd for $C_{26}H_{34}N_3O_3$ $[M + H]^+$, 436.2600; found, 436.2622.

■ ASSOCIATED CONTENT

Supporting Information

Synthesis and characterization of **6**−**8**; additional spectroscopic, kinetic, computational, and X-ray crystallographic data. This material is available free of charge via the Internet at http://pubs.acs.org.

■ AUTHOR INFORMATION

Corresponding Author

dongwhan@indiana.edu

Notes

The authors declare no competing financial interest.

■ ACKNOWLEDGMENTS

This work was supported by DTRA/ARO (W911NF-07-1-0533).

■ REFERENCES

(1) (a) Jencks, W. P. *Catalysis in Chemistry and Enzymology*; McGraw-Hill: New York, 1969. (b) Berg, J. M.; Tymoczko, J. L.; Stryer, L. *Biochemistry*; 7th ed.; W. H. Freeman and Company: New York, 2012.

(2) (a) Lippard, S. J.; Berg, J. M. *Principles of Bioinorganic Chemistry*; University Science Books: Mill Valley, CA, 1994. (b) *Concepts and Models in Bioinorganic Chemistry*; Kraatz, H.-B.; Metzler-Nolte, N., Eds.; Wiley-VCH: Weinheim, 2006. (c) *Activation of Small Molecules: Organometallic and Bioinorganic Perspectives*; Tolman, W. B., Ed.; Wiley-VCH: Weinheim, 2006. (d) *Biological Inorganic Chemistry: Structure & Reactivity*; Bertini, I.; Gray, H. B.; Stiefel, E. I.; Valentine, J. S., Eds.; University Science Books: Sausalito, CA, 2007.

(3) Jeffrey, G. A.; Saenger, W. *Hydrogen bonding in biological structures*; Springer-Verlag: Berlin, 1991.

(4) (a) Hedstrom, L. *Chem. Rev.* **2002**, *102*, 4501−4524. (b) Ekici, O. D.; Paetzel, M.; Dalbey, R. E. *Protein Sci.* **2008**, *17*, 2023−2037.

(5) *Hydrogen Bonding in Organic Synthesis*; Pihko, P. M., Ed.; Wiley−VCH: Weinheim, 2009.

(6) (a) Schenker, S.; Zamfir, A.; Freund, M.; Tsogoeva, S. B. *Eur. J. Org. Chem.* **2011**, 2209−2222. (b) Sohtome, Y.; Nagasawa, K. *Synlett* **2010**, 1−22. (c) Knowles, R. R.; Jacobsen, E. N. *Proc. Natl. Acad. Sci. U.S.A.* **2010**, *107*, 20678−20685. (d) Doyle, A. G.; Jacobsen, E. N. *Chem. Rev.* **2007**, *107*, 5713−5743. (e) Akiyama, T. *Chem. Rev.* **2007**, *107*, 5744−5758. (f) Ting, A.; Schaus, S. E. *Eur. J. Org. Chem.* **2007**, 5797−5815. (g) Taylor, M. S.; Jacobsen, E. N. *Angew. Chem., Int. Ed.* **2006**, *45*, 1520−1543. (h) Connon, S. J. *Chem.—Eur. J.* **2006**, *12*, 5418−5427. (i) Connon, S. J. *Angew. Chem., Int. Ed.* **2006**, *45*, 3909−3912. (j) Akiyama, T.; Itoh, J.; Fuchibe, K. *Adv. Synth. Catal.* **2006**, *348*, 999−1010. (k) Pihko, P. M. *Angew. Chem., Int. Ed.* **2004**, *43*, 2062−2064.

(7) Huynh, P. N. H.; Walvoord, R. R.; Kozlowski, M. C. *J. Am. Chem. Soc.* **2012**, *134*, 15621−15623.

(8) (a) Sigman, M. S.; Jacobsen, E. N. *J. Am. Chem. Soc.* **1998**, *120*, 4901−4902. (b) Vachal, P.; Jacobsen, E. N. *J. Am. Chem. Soc.* **2002**, *124*, 10012−10014. (c) Zuend, S. J.; Jacobsen, E. N. *J. Am. Chem. Soc.* **2007**, *129*, 15872−15883. (d) Zuend, S. J.; Jacobsen, E. N. *J. Am. Chem. Soc.* **2009**, *131*, 15358−15374.

(9) In this chemistry, the ground-state complex between the catalyst and the electrophile can take multiple reaction pathways, including direct attack of CN^- to the (thio)urea-bound imine/ketone group or delivery of the (thio)urea-bound CN^- to the imine/ketone group in the enantioselectivity-determining step.[8c,d]

(10) Taylor, J. E.; Bull, S. D.; Williams, J. M. J. *Chem. Soc. Rev.* **2012**, *41*, 2109−2121.

(11) (a) Simón, L.; Goodman, J. M. *J. Am. Chem. Soc.* **2012**, *134*, 16869−16876. (b) Uyeda, C.; Jacobsen, E. N. *J. Am. Chem. Soc.* **2011**, *133*, 5062−5075. (c) Ube, H.; Shimada, N.; Terada, M. *Angew. Chem., Int. Ed.* **2010**, *49*, 1858−1861. (d) Misaki, T.; Takimoto, G.; Sugimura, T. *J. Am. Chem. Soc.* **2010**, *132*, 6286−6287. (e) Dong, S.; Liu, X.; Chen, X.; Mei, F.; Zhang, Y.; Gao, B.; Lin, L.; Feng, X. *J. Am. Chem. Soc.* **2010**, *132*, 10650−10651. (f) Liu, H.; Leow, D.; Huang, K.-W.; Tan, C.-H. *J. Am. Chem. Soc.* **2009**, *131*, 7212−7213. (g) Yu, Z.; Liu, X.; Zhou, L.; Lin, L.; Feng, X. *Angew. Chem., Int. Ed.* **2009**, *48*, 5195−5198. (h) Chuma, A.; Horn, H. W.; Swope, W. C.; Pratt, R. C.; Zhang, L.; Lohmeijer, B. G. G.; Wade, C. G.; Waymouth, R. M.; Hedrick, J. L.; Rice, J. E. *J. Am. Chem. Soc.* **2008**, *130*, 6749−6754. (i) Terada, M.; Ikehara, T.; Ube, H. *J. Am. Chem. Soc.* **2007**, *129*, 14112−14113. (j) Shen, J.; Nguyen, T. T.; Goh, Y.-P.; Ye, W.; Fu, X.; Xu, J.; Tan, C.-H. *J. Am. Chem. Soc.* **2006**, *128*, 13692−13693. (k) Ishikawa, T.; Isobe, T. *Chem.—Eur. J.* **2002**, *8*, 552−557. (l) Kita, T.; Georgieva, A.; Hashimoto, Y.; Nakata, T.; Nagasawa, K. *Angew. Chem., Int. Ed.* **2002**, *41*, 2832−2834. (m) Corey, E. J.; Grogan, M. J. *Org. Lett.* **1999**, *1*, 157−160.

(12) *Superbases for Organic Synthesis: Guanidines, Amidines, Phosphazines and Related Organocatalysts*; Ishikawa, T., Ed.; Wiley: New York, 2009.

(13) Maksić, Z. B.; Kovačević, B.; Vianello, R. *Chem. Rev.* **2012**, *112*, 5240−5270.

(14) (a) Kunetskiy, R. A.; Polyakova, S. M.; Vavřík, J.; Císařová, I.; Saame, J.; Nerut, E. R.; Koppel, I.; Koppel, I. A.; Kütt, A.; Leito, I.; Lyapkalo, I. M. *Chem.—Eur. J.* **2012**, *18*, 3621−3630. (b) Coles, M. P.; Aragón-Sáez, P. J.; Oakley, S. H.; Hitchcock, P. B.; Davidson, M. G.; Maksić, Z. B.; Vianello, R.; Leito, I.; Kaljurand, I.; Apperley, D. C. *J. Am. Chem. Soc.* **2009**, *131*, 16858−16868. (c) Raab, V.; Kipke, J.; Gschwind, R. M.; Sundermeyer, J. *Chem.—Eur. J.* **2002**, *8*, 1682−1693. (d) Ishikawa, T.; Araki, Y.; SKumamoto, T.; Seki, H.; Fukuda, K.; Isobe, T. *Chem. Commun.* **2001**, 245−246. (e) Isobe, T.; Fukuda, K.; Araki, Y.; Ishikawa, T. *Chem. Commun.* **2001**, 243−244. (f) Maksić, Z. B.; Kovačević, B. *J. Org. Chem.* **2000**, *65*, 3303−3309. (g) Costa, M.; Paolo Chiusoli, G.; Taffurelli, D.; Dalmonego, G. *J. Chem. Soc., Perkin Trans. 1* **1998**, 1541−1546.

(15) (a) Yonke, B. L.; Keane, A. J.; Zavalij, P. Y.; Sita, L. R. *Organometallics* **2012**, *31*, 345−355. (b) Chen, S.-J.; Dougan, B. A.; Chen, X.-T.; Xue, Z.-L. *Organometallics* **2012**, *31*, 3443−3446. (c) Panda, T. K.; Tsurugi, H.; Pal, K.; Kaneko, H.; Mashima, K. *Organometallics* **2009**, *29*, 34−37. (d) Zhang, J.; Han, F.; Han, Y.; Chen, Z.; Zhou, X. *Dalton Trans.* **2009**, 1806−1811. (e) Jones, C.; Junk, P. C.; Platts, J. A.; Stasch, A. *J. Am. Chem. Soc.* **2006**, *128*, 2206−2207. (f) Trifonov, A. A.; Skvortsov, G. G.; Lyubov, D. M.;

Skorodumova, N. A.; Fukin, G. K.; Baranov, E. V.; Glushakova, V. N. *Chem.—Eur. J.* **2006**, *12*, 5320−5327. (g) Rische, D.; Baunemann, A.; Winter, M.; Fischer, R. A. *Inorg. Chem.* **2005**, *45*, 269−277. (h) Wilder, C. B.; Reitfort, L. L.; Abboud, K. A.; McElwee-White, L. *Inorg. Chem.* **2005**, *45*, 263−268. (i) Carmalt, C. J.; Newport, A. C.; O'Neill, S. A.; Parkin, I. P.; White, A. J. P.; Williams, D. J. *Inorg. Chem.* **2005**, *44*, 615−619. (j) Bailey, P. J.; Pace, S. *Coord. Chem. Rev.* **2001**, *214*, 91−141. (k) Bailey, P. J.; Grant, K. J.; Mitchell, L. A.; Pace, S.; Parkin, A.; Parsons, S. *J. Chem. Soc., Dalton Trans.* **2000**, 1887−1891. (l) Maia, J. R. d. S.; Gazard, P. A.; Kilner, M.; Batsanov, A. S.; Howard, J. A. K. *J. Chem. Soc., Dalton Trans.* **1997**, 4625−4630.

(16) Schmuck, C.; Kuchelmeister, H. Y. In *Artificial Receptors for Chemical Sensors*; Wiley−VCH: Weinheim, 2010, pp 273−317.

(17) (a) Kubik, S. *Chem. Soc. Rev.* **2009**, *38*, 585−605. (b) Blondeau, P.; Segura, M.; Pérez-Fernández, R.; de Mendoza, J. *Chem. Soc. Rev.* **2007**, *36*, 198−210. (c) Schug, K. A.; Lindner, W. *Chem. Rev.* **2005**, *105*, 67−114.

(18) (a) Best, M. D.; Tobey, S. L.; Anslyn, E. V. *Coord. Chem. Rev.* **2003**, *240*, 3−15. (b) Tobey, S. L.; Anslyn, E. V. *J. Am. Chem. Soc.* **2003**, *125*, 14807−14815. (c) Metzger, A.; Lynch, V. M.; Anslyn, E. V. *Angew. Chem., Int. Ed.* **1997**, *36*, 862−865.

(19) (a) Baldini, L.; Cacciapaglia, R.; Casnati, A.; Mandolini, L.; Salvio, R.; Sansone, F.; Ungaro, R. *J. Org. Chem.* **2012**, *77*, 3381−3389. (b) Sansone, F.; Dudič, M.; Donofrio, G.; Rivetti, C.; Baldini, L.; Casnati, A.; Cellai, S.; Ungaro, R. *J. Am. Chem. Soc.* **2006**, *128*, 14528−14536. (c) Sun, Y.; Zhong, C.; Gong, R.; Fu, E. *Orga. Biomol. Chem.* **2008**, *6*, 3044−3047. (d) Jiménez Blanco, J. L.; Bootello, P.; Benito, J. M.; Ortiz Mellet, C.; García Fernández, J. M. *J. Org. Chem.* **2006**, *71*, 5136−5143.

(20) (a) Avinash, M. B.; Verheggen, E.; Schmuck, C.; Govindaraju, T. *Angew. Chem., Int. Ed.* **2012**, *51*, 10324−10328. (b) Gröger, G.; Meyer-Zaika, W.; Böttcher, C.; Gröhn, F.; Ruthard, C.; Schmuck, C. *J. Am. Chem. Soc.* **2011**, *133*, 8961−8971. (c) Gröger, G.; Stepanenko, V.; Würthner, F.; Schmuck, C. *Chem. Commun.* **2009**, 698−700. (d) Schmuck, C.; Rehm, T.; Gröhn, F.; Klein, K.; Reinhold, F. *J. Am. Chem. Soc.* **2006**, *128*, 1430−1431. (e) Lam, C.-K.; Xue, F.; Zhang, J.-P.; Chen, X.-M.; Mak, T. C. W. *J. Am. Chem. Soc.* **2005**, *127*, 11536−11537. (f) Prabhakaran, P.; Puranik, V. G.; Sanjayan, G. J. *J. Org. Chem.* **2005**, *70*, 10067−10072. (g) Schmuck, C.; Wienand, W. *J. Am. Chem. Soc.* **2003**, *125*, 452−459. (h) Videnova-Adrabińska, V.; Turowska-Tyrk, I.; Borowiak, T.; Dutkiewicz, G. *New J. Chem.* **2001**, *25*, 1403−1409.

(21) (a) You, Y.-C.; Tzeng, M.-C.; Lai, C.-C.; Chiu, S.-H. *Org. Lett.* **2012**, *14*, 1046−1049. (b) Lin, T.-C.; Lai, C.-C.; Chiu, S.-H. *Org. Lett.* **2009**, *11*, 613−616.

(22) (a) Wiberg, K. B. *J. Am. Chem. Soc.* **1990**, *112*, 4177−4182. (b) Gobbi, A.; Frenking, G. *J. Am. Chem. Soc.* **1993**, *115*, 2362−2372. (c) Göbel, M.; Klapötke, T. M. *Chem. Commun.* **2007**, 3180−3182. (d) Yamada, T.; Liu, X.; Englert, U.; Yamane, H.; Dronskowski, R. *Chem.—Eur. J.* **2009**, *15*, 5651−5655.

(23) (a) Niebling, S.; Srivastava, S. K.; Herrmann, C.; Wich, P. R.; Schmuck, C.; Schlucker, S. *Chem. Commun.* **2010**, *46*, 2133−2135. (b) Urban, C.; Schmuck, C. *Chem.—Eur. J.* **2010**, *16*, 9502−9510. (c) Schmuck, C.; Dudaczek, J. *Eur. J. Org. Chem.* **2007**, *2007*, 3326−3330. (d) Schmuck, C.; Hernandez-Folgado, L. *Org. Biomol. Chem.* **2007**, *5*, 2390−2394. (e) Schmuck, C.; Schwegmann, M. *Org. Lett.* **2005**, *7*, 3517−3520. (f) Schlund, S.; Schmuck, C.; Engels, B. *J. Am. Chem. Soc.* **2005**, *127*, 11115−11124. (g) Schmuck, C.; Geiger, L. *J. Am. Chem. Soc.* **2004**, *126*, 8898−8899.

(24) (a) Sibanda, B. L.; Blundell, T. L.; Thornton, J. M. *J. Mol. Biol.* **1989**, *206*, 759−777. (b) Burgess, K. *Acc. Chem. Res.* **2001**, *34*, 826−835. (c) Robinson, J. A. *Acc. Chem. Res.* **2008**, *41*, 1278−1288.

(25) For representative examples of synthetic mimics of peptide β-turn, see: (a) Nowick, J. S. *Org. Biomol. Chem.* **2006**, *4*, 3869−3885. (b) Loughlin, W. A.; Tyndall, J. D. A.; Glenn, M. P.; Fairlie, D. P. *Chem. Rev.* **2004**, *104*, 6085−6118. (c) Kemp, D. S.; Bowen, B. R.; Muendel, C. C. *J. Org. Chem.* **1990**, *55*, 4650−4657. (d) Kemp, D. S.; Li, Z. Q. *Tetrahedron Lett.* **1995**, *36*, 4175−4178. (e) Kemp, D. S.; Li, Z. Q. *Tetrahedron Lett.* **1995**, *36*, 4179−4180. (f) Diaz, H.; Espina, J. R.; Kelly, J. W. *J. Am. Chem. Soc.* **1992**, *114*, 8316−8318. (g) Smith, A. B., III; Guzman, M. C.; Sprengeler, P. A.; Keenan, T. P.; Holcomb, R. C.; Wood, J. L.; Carroll, P. J.; Hirschmann, R. *J. Am. Chem. Soc.* **1994**, *116*, 9947−9962. (h) Brandmeier, V.; Sauer, W. H. B.; Feigel, M. *Helv. Chim. Acta* **1994**, *77*, 70−85. (i) Ogawa, M. Y.; Gretchikhine, A. B.; Soni, S.-D.; Davis, S. M. *Inorg. Chem.* **1995**, *34*, 6423−6424. (j) Hanessian, S.; McNaughton-Smith, G.; Lombart, H.-G.; Lubell, W. D. *Tetrahedron* **1997**, *53*, 12789−12854. (k) Wyrembak, P. N.; Hamilton, A. D. *J. Am. Chem. Soc.* **2009**, *131*, 4566−4567.

(26) Jo, J.; Lee, D. *J. Am. Chem. Soc.* **2009**, *131*, 16283−16291.

(27) (a) Lim, M. H.; Lippard, S. J. *Acc. Chem. Res.* **2007**, *40*, 41−51. (b) Nolan, E. M.; Lippard, S. J. *Acc. Chem. Res.* **2009**, *42*, 193−203. (c) Kim, H. N.; Lee, M. H.; Kim, H. J.; Kim, J. S.; Yoon, J. *Chem. Soc. Rev.* **2008**, *37*, 1465−1472. (d) Kobayashi, H.; Ogawa, M.; Alford, R.; Choyke, P. L.; Urano, Y. *Chem. Rev.* **2010**, *110*, 2620−2640. (e) Han, J.; Burgess, K. *Chem. Rev.* **2010**, *110*, 2709−2728. (f) Quang, D. T.; Kim, J. S. *Chem. Rev.* **2010**, *110*, 6280−6301. (g) Lippert, A. R.; Van de Bittner, G. C.; Chang, C. J. *Acc. Chem. Res.* **2011**, *44*, 793−804. (h) Chen, X.; Pradhan, T.; Wang, F.; Kim, J. S.; Yoon, J. *Chem. Rev.* **2012**, *112*, 1910−1956.

(28) (a) Shieh, P.; Hangauer, M. J.; Bertozzi, C. R. *J. Am. Chem. Soc.* **2012**, *134*, 17428−17431. (b) Kurishita, Y.; Kohira, T.; Ojida, A.; Hamachi, I. *J. Am. Chem. Soc.* **2012**, *134*, 18779−18789. (c) Abo, M.; Urano, Y.; Hanaoka, K.; Terai, T.; Komatsu, T.; Nagano, T. *J. Am. Chem. Soc.* **2011**, *133*, 10629−10637. (d) Dickinson, B. C.; Huynh, C.; Chang, C. J. *J. Am. Chem. Soc.* **2010**, *132*, 5906−5915. (e) Ojida, A.; Takashima, I.; Kohira, T.; Nonaka, H.; Hamachi, I. *J. Am. Chem. Soc.* **2008**, *130*, 12095−12101. (f) Ahn, Y.-H.; Lee, J.-S.; Chang, Y.-T. *J. Am. Chem. Soc.* **2007**, *129*, 4510−4511. (g) Urano, Y.; Kamiya, M.; Kanda, K.; Ueno, T.; Hirose, K.; Nagano, T. *J. Am. Chem. Soc.* **2005**, *127*, 4888−4894.

(29) (a) Clayden, J.; Lund, A.; Vallverdú, L.; Helliwell, M. *Nature* **2004**, *431*, 966−971. (b) Morisaki, Y.; Murakami, T.; Sawamura, T.; Chujo, Y. *Macromolecules* **2009**, *42*, 3656−3660. (c) Morisaki, Y.; Fernandes, J. A.; Wada, N.; Chujo, Y. *J. Polym. Sci., Part A: Polym. Chem.* **2009**, *47*, 4279−4288. (d) Morisaki, Y.; Sawamura, T.; Murakami, T.; Chujo, Y. *Org. Lett.* **2010**, *12*, 3188−3191. (e) Fernandes, J. A.; Morisaki, Y.; Chujo, Y. *Polym. J.* **2011**, *43*, 733−737. (f) Chen, Q.; Wang, J.-X.; Wang, Q.; Bian, N.; Li, Z.-H.; Yan, C.-G.; Han, B.-H. *Macromolecules* **2011**, *44*, 7987−7993.

(30) (a) Rosenthal, J.; Nocera, D. G. *Acc. Chem. Res.* **2007**, *40*, 543−553. (b) Dogutan, D. K.; McGuire, R.; Nocera, D. G. *J. Am. Chem. Soc.* **2011**, *133*, 9178−9180. (c) Lee, C. H.; Dogutan, D. K.; Nocera, D. G. *J. Am. Chem. Soc.* **2011**, *133*, 8775−8777. (d) Dogutan, D. K.; Stoian, S. A.; McGuire, R.; Schwalbe, M.; Teets, T. S.; Nocera, D. G. *J. Am. Chem. Soc.* **2010**, *133*, 131−140. (e) Dogutan, D. K.; Bediako, D. K.; Teets, T. S.; Schwalbe, M.; Nocera, D. G. *Org. Lett.* **2010**, *12*, 1036−1039.

(31) (a) Birkholz, M.-N.; Freixa, Z.; van Leeuwen, P. W. N. M. *Chem. Soc. Rev.* **2009**, *38*, 1099−1118. (b) Chikkali, S. H.; Bellini, R.; Berthon-Gelloz, G.; van der Vlugt, J. I.; Bruin, B. d.; Reek, J. N. H. *Chem. Commun.* **2010**, *46*, 1244−1246. (c) Kadish, K. M.; Fremond, L.; Shen, J.; Chen, P.; Ohkubo, K.; Fukuzumi, S.; El Ojaimi, M.; Gros, C. P.; Barbe, J.-M.; Guilard, R. *Inorg. Chem.* **2009**, *48*, 2571−2582. (d) Piesik, D. F. J.; Haack, P.; Harder, S.; Limberg, C. *Inorg. Chem.* **2009**, *48*, 11259−11264. (e) Guo, Z.; Tong, W.-L.; Chan, M. C. W. *Chem. Commun.* **2009**, 6189−6191. (f) Minglana, J. J. G.; Okazaki, M.; Hasegawa, K.; Luh, L.-S.; Yamahira, N.; Komuro, T.; Ogino, H.; Tobita, H. *Organometallics* **2007**, *26*, 5859−5866. (g) Mora, G.; Deschamps, B.; van Zutphen, S.; Le Goff, X. F.; Ricard, L.; Le Floch, P. *Organometallics* **2007**, *26*, 1846−1855. (h) Kadish, K. M.; Fremond, L.; Ou, Z.; Shao, J.; Shi, C.; Anson, F. C.; Burdet, F.; Gros, C. P.; Barbe, J.-M.; Guilard, R. *J. Am. Chem. Soc.* **2005**, *127*, 5625−5631.

(32) (a) Nowick, J. S.; Ballester, P.; Ebmeyer, F.; Rebek, J., Jr. *J. Am. Chem. Soc.* **1990**, *112*, 8902−8906. (b) Park, T. K.; Schroeder, J.; Rebek, J., Jr. *J. Am. Chem. Soc.* **1991**, *113*, 5125−5127. (c) Shipps, G.; Rebek, J., Jr. *Tetrahedron Lett.* **1994**, *35*, 6823−6826. (d) Kamioka, S.; Ajami, D.; Rebek, J., Jr. *Chem. Commun.* **2009**, 7324−7326. (e) Kamioka, S.; Ajami, D.; Rebek, J., Jr. *Proc. Natl. Acad. Sci. U.S.A.*

2010, *107*, 541−544. (f) Deans, R.; Niemz, A.; Breinlinger, E. C.; Rotello, V. M. *J. Am. Chem. Soc.* **1997**, *119*, 10863−10864. (g) MacGillivray, L. R.; Siebke, M. M.; Reid, J. L. *Org. Lett.* **2001**, *3*, 1257−1260. (h) Skene, W. G.; Berl, V.; Risler, H.; Khoury, R.; Lehn, J.-M. *Org. Biomol. Chem.* **2006**, *4*, 3652−3663.

(33) Shankaramma, S. C.; Athanassiou, Z.; Zerbe, O.; Moehle, K.; Mouton, C.; Bernardini, F.; Vrijbloed, J. W.; Obrecht, D.; Robinson, J. A. *ChemBioChem* **2002**, *3*, 1126−1133.

(34) (a) El-Sayed, M. A. *Acc. Chem. Res.* **1968**, *1*, 8−16. (b) Turro, N. J. *Modern Molecular Photochemistry*; University Science Books: Sausalito, CA, 1991. (c) de Silva, A. P.; Gunaratne, H. Q. N.; Gunnlaugsson, T.; Huxley, A. J. M.; McCoy, C. P.; Rademacher, J. T.; Rice, T. E. *Chem. Rev.* **1997**, *97*, 1515−1566.

(35) The C−N distances of 1.301(3) and 1.304(3) Å determined for the C29−N2 and C29−N3 bond, respectively, of the guanidyl group are comparable to each other but significantly shorter than that (1.397(3) Å) of C29−N1, which is also consistent with charge delocalization upon protonation at the N2 position. Attempts to obtain single crystals of the conjugate base **1** were less successful.

(36) (a) Pranata, J.; Wierschke, S. G.; Jorgensen, W. L. *J. Am. Chem. Soc.* **1991**, *113*, 2810−2819. (b) Schneider, H.-J.; Yatsimirsky, A. *Principles and Methods in Supramolecular Chemistry*; John Wiley & Sons: Chichester, U.K., 2000.

(37) Schmuck, C.; Wienand, W. *J. Am. Chem. Soc.* **2002**, *125*, 452−459.

(38) Laeckmann, D.; Rogister, F.; Dejardin, J.-V.; Prosperi-Meys, C.; Géczy, J.; Delarge, J.; Masereel, B. *Bioorg. Med. Chem.* **2002**, *10*, 1793−1804.

(39) Kleinmaier, R.; Keller, M.; Igel, P.; Buschauer, A.; Gschwind, R. M. *J. Am. Chem. Soc.* **2010**, *132*, 11223−11233.

(40) (a) Gilli, G.; Gilli, P. *The Nature of the Hydrogen Bond*; Oxford University Press: New York, 2009. (b) Gilli, P.; Pretto, L.; Bertolasi, V.; Gilli, G. *Acc. Chem. Res.* **2009**, *42*, 33−44.

(41) Abraham, R. J.; Mobli, M.; Smith, R. J. *Magn. Reson. Chem.* **2003**, *41*, 26−36.

(42) (a) Deetz, M. J.; Fahey, J. E.; Smith, B. D. *J. Phys. Org. Chem.* **2001**, *14*, 463−467. (b) Modarresi-Alam, A. R.; Najafi, P.; Rostamizadeh, M.; Keykha, H.; Bijanzadeh, H.-R.; Kleinpeter, E. *J. Org. Chem.* **2007**, *72*, 2208−2211. (c) Hayashi, K.; Matubayasi, N.; Jiang, C.; Yoshimura, T.; Majumdar, S.; Sasamori, T.; Tokitoh, N.; Kawabata, T. *J. Org. Chem.* **2010**, *75*, 5031−5036.

(43) (a) Greenhill, J. V.; Ismail, M. J.; Bedford, G. R.; Edwards, P. N.; Taylor, P. J. *J. Chem. Soc., Perkin Trans. 2* **1985**, 1265−1274. (b) Greenhill, J. V.; Ismail, M. J.; Edwards, P. N.; Taylor, P. J. *J. Chem. Soc., Perkin Trans. 2* **1985**, 1255−1264.

(44) (a) Reichardt, C. *Chem. Rev.* **1994**, *94*, 2319−2358. (b) Reichardt, C.; Welton, T. *Solvents and Solvent Effects in Organic Chemistry*; 4th ed.; Wiley-VCH: Weinheim, 2010. (c) Carey, F. A.; Sundberg, R. J. *Advanced Organic Chemistry, Part A: Structure and Mechanisms*; 5th ed.; Springer: New York, 2007.

(45) *Chemical Reactivity and Reaction Paths*; Klopman, G., Ed.; Wiley: New York, 1974.

(46) (a) Klopman, G. *J. Am. Chem. Soc.* **1968**, *90*, 223−234. (b) Parr, R. G.; Yang, W. *J. Am. Chem. Soc.* **1984**, *106*, 4049−4050.

(47) For previous examples of Fukui function analysis used in the theoretical investigation of nucleophilic addition to carbonyl groups, see: (a) Méndez, F.; Galván, M.; Garritz, A.; Vela, A.; Gàzquez, J. *J. Mol. Str.* **1992**, *277*, 81−86. (b) Roy, R. K.; Krishnamurti, S.; Geerlings, P.; Pal, S. *J. Phys. Chem. A.* **1998**, *102*, 3746−3755. (c) Roy, R. K.; Choho, K.; De Proft, F.; Geerlings, P. *J. Phys. Org. Chem.* **1999**, *12*, 503−509.

(48) The only exception is $[\mathbf{1}'\cdot H]^+_t$, for which the LUMO is located at the positively charged guanidinyl end. In this case, LUMO+1 has significant contribution of the aldehyde π^* MO, which was compared with the LUMO of the rest of the series of the DFT models.

(49) Meot-Ner Mautner, M. *Chem. Rev.* **2005**, *105*, 213−284.

(50) (a) Badugu, R.; Lakowicz, J. R.; Geddes, C. D. *J. Am. Chem. Soc.* **2005**, *127*, 3635−3641. (b) Huh, J. O.; Do, Y.; Lee, M. H. *Organometallics* **2008**, *27*, 1022−1025. (c) Agou, T.; Sekine, M.; Kobayashi, J.; Kawashima, T. *Chem.—Eur. J.* **2009**, *15*, 5056−5062. (d) Jamkratoke, M.; Ruangpornvisuti, V.; Tumcharern, G.; Tuntulani, T.; Tomapatanaget, B. *J. Org. Chem.* **2009**, *74*, 3919−3922.

(51) (a) Hudnall, T. W.; Gabbaï, F. P. *J. Am. Chem. Soc.* **2007**, *129*, 11978−11986. (b) Kim, Y.; Zhao, H.; Gabbaï, F. P. *Angew. Chem., Int. Ed.* **2009**, *48*, 4957−4960. (c) Kim, Y.; Huh, H.-S.; Lee, M. H.; Lenov, I. L.; Zhao, H.; Gabbaï, F. P. *Chem.—Eur. J.* **2011**, *17*, 2057−2062.

(52) (a) Kim, Y.-H.; Hong, J.-I. *Chem. Commun.* **2002**, 512−513. (b) Lee, J. H.; Jeong, A. R.; Shin, I.-S.; Kim, H.-J.; Hong, J.-I. *Org. Lett.* **2010**, *12*, 764−767. (c) Chow, C.-F.; Lam, M. H. W.; Wong, W.-Y. *Inorg. Chem.* **2004**, *43*, 8387−8393. (d) Liu, Y.; Lv, X.; Zhao, Y.; Liu, J.; Sun, Y.-Q.; Wang, P.; Guo, W. *J. Mater. Chem.* **2012**, *22*, 1747−1750.

(53) For a recent review on this topic, see: Lou, X.; Ou, D.; Li, Q.; Li, Z. *Chem. Commun.* **2012**, *48*, 8462−8477.

(54) (a) Zeng, Q.; Cai, P.; Li, Z.; Qin, J.; Tang, B. Z. *Chem. Commun.* **2008**, 1094−1096. (b) Li, Z. a.; Lou, X.; Yu, H.; Li, Z.; Qin, J. *Macromolecules* **2008**, *41*, 7433−7439. (c) Touceda-Varela, A.; Stevenson, E. I.; Galve-Gasión, J. A.; Dryden, D. T. F.; Mareque-Rivas, J. C. *Chem. Commun.* **2008**, 1998−2000. (d) Shang, L.; Zhang, L.; Dong, S. *Analyst* **2009**, *134*, 107−113. (e) Chung, S.-Y.; Nam, S.-W.; Lim, J.; Park, S.; Yoon, J. *Chem. Commun.* **2009**, 2866−2868. (f) Divya, K. P.; Sreejith, S.; Balakrishna, B.; Jayamurthy, P.; Anees, P.; Ajayaghosh, A. *Chem. Commun.* **2010**, *46*, 6069−6071. (g) Chen, X.; Nam, S.-W.; Kim, G.-H.; Song, N.; Jeong, Y.; Shin, I.; Kim, S. K.; Kim, J.; Park, S.; Yoon, J. *Chem. Commun.* **2010**, *46*, 8953−8955. (h) Jung, H. S.; Han, J. H.; Kim, Z. H.; Kang, C.; Kim, J. S. *Org. Lett.* **2011**, *13*, 5056−5059. (i) Gee, H.-C.; Lee, C.-H.; Jeong, Y.-H.; Jang, W.-D. *Chem. Commun.* **2011**, *47*, 11963−11965. (j) Xu, J.-F.; Chen, H.-H.; Chen, Y.-Z.; Li, Z.-J.; Wu, L.-Z.; Tung, C.-H.; Yang, Q.-Z. *Sens. Actuators B* **2012**, *168*, 14−19. (k) Xie, Y.; Ding, Y.; Li, X.; Wang, C.; Hill, J. P.; Ariga, K.; Zhang, W.; Zhu, W. *Chem. Commun.* **2012**, *48*, 11513−11515.

(55) (a) Ros-Lis, J. V.; Martínez-Máñez, R.; Soto, J. *Chem. Commun.* **2002**, 2248−2249. (b) García, F.; García, J. M.; García-Acosta, B.; Martínez-Máñez, R.; Sancenón, F.; Soto, J. *Chem. Commun.* **2005**, 2790−2792. (c) Tomasulo, M.; Raymo, F. M. *Org. Lett.* **2005**, *7*, 4633−4636. (d) Tomasulo, M.; Sortino, S.; White, A. J. P.; Raymo, F. M. *J. Org. Chem.* **2006**, *71*, 744−753. (e) Yang, Y.-K.; Tae, J. *Org. Lett.* **2006**, *8*, 5721−5723. (f) Chung, Y.; Lee, H.; Ahn, K. H. *J. Org. Chem.* **2006**, *71*, 9470−9474. (g) Lee, K.-S.; Lee, J. T.; Hong, J.-I.; Kim, H.-J. *Chem. Lett.* **2007**, *36*, 816−817. (h) Ekmekci, Z.; Yilmaz, M. D.; Akkaya, E. U. *Org. Lett.* **2008**, *10*, 461−464. (i) Niu, H.-T.; Su, D.; Jiang, X.; Yang, W.; Yin, Z.; He, J.; Cheng, J.-P. *Org. Biomol. Chem.* **2008**, *6*, 3038−3040. (j) Cho, D.-G.; Kim, J. H.; Sessler, J. L. *J. Am. Chem. Soc.* **2008**, *130*, 12163−12167. (k) Niu, H.-T.; Jiang, X.; He, J.; Cheng, J.-P. *Tetrahedron Lett.* **2008**, *49*, 6521−6524. (l) Hong, S.-J.; Yoo, J.; Kim, S.-H.; Kim, J. S.; Yoon, J.; Lee, C.-H. *Chem. Commun.* **2009**, 189−191. (m) Liu, Z.; Wang, X.; Yang, Z.; He, W. *J. Org. Chem.* **2011**, *76*, 10286−10290.

(56) (a) Shiraishi, Y.; Sumiya, S.; Hirai, T. *Chem. Commun.* **2011**, *47*, 4953−4955. (b) Shiraishi, Y.; Sumiya, S.; Manabe, K.; Hirai, T. *ACS Appl. Mater. Interfaces* **2011**, *3*, 4649−4656. (c) Sessler, J. L.; Cho, D.-G. *Org. Lett.* **2008**, *10*, 73−75. (d) Park, S.; Kim, H.-J. *Chem. Commun.* **2010**, *46*, 9197−9199. (e) Kim, G.-J.; Kim, H.-J. *Tetrahedron Lett.* **2010**, *51*, 185−187. (f) Lee, H.; Kim, H.-J. *Tetrahedron Lett.* **2012**, *53*, 5455−5457. (g) Lin, Y.-D.; Peng, Y.-S.; Su, W.; Tu, C.-H.; Sun, C.-H.; Chow, T. J. *Tetrahedron* **2012**, *68*, 2523−2526. (h) Cheng, X.; Tang, R.; Jia, H.; Feng, J.; Qin, J.; Li, Z. *ACS Appl. Mater. Interfaces* **2012**, *4*, 4387−4392. (i) Lee, C.-H.; Yoon, H.-J.; Shim, J.-S.; Jang, W.-D. *Chem. − Eur. J.* **2012**, *18*, 4513−4516. (j) Chung, Y. M.; Raman, B.; Kim, D.-S.; Ahn, K. H. *Chem. Commun.* **2006**, 186−188. (k) Miyaji, H.; Kim, D.-S.; Chang, B.-Y.; Park, E.; Park, S.-M.; Ahn, K. H. *Chem. Commun.* **2008**, 753−755. (l) Chen, C.-L.; Chen, Y.-H.; Chen, C.-Y.; Sun, S.-S. *Org. Lett.* **2006**, *8*, 5053−5056. (m) Lee, K.-S.; Kim, H.-J.; Kim, G.-H.; Shin, I.; Hong, J.-I. *Org. Lett.* **2008**, *10*, 49−51. (n) Kwon, S. K.; Kou, S.; Kim, H. N.; Chen, X.; Hwang, H.; Nam, S.-W.; Kim, S. H.; Swamy, K. M. K.; Park, S.; Yoon, J. *Tetrahedron Lett.* **2008**, *49*, 4102−4105. (o) Yu, H.; Zhao, Q.; Jiang, Z.; Qin, J.; Li, Z. *Sens. Actuators B* **2010**,

148, 110−116. (p) Li, H.; Li, B.; Jin, L.-Y.; Kan, Y.; Yin, B. *Tetrahedron* **2011**, *67*, 7348−7353. (q) Lv, X.; Liu, J.; Liu, Y.; Zhao, Y.; Chen, M.; Wang, P.; Guo, W. *Sens. Actuators B* **2011**, *158*, 405−410. (r) Lv, X.; Liu, J.; Liu, Y.; Zhao, Y.; Chen, M.; Wang, P.; Guo, W. *Org. Biomol. Chem.* **2011**, *9*, 4954−4958. (s) Lv, X.; Liu, J.; Liu, Y.; Zhao, Y.; Sun, Y.-Q.; Wang, P.; Guo, W. *Chem. Commun.* **2011**, *47*, 12843−12845. (t) Kim, H. J.; Ko, K. C.; Lee, J. H.; Lee, J. Y.; Kim, J. S. *Chem. Commun.* **2011**, *47*, 2886−2888. (u) Mashraqui, S. H.; Betkar, R.; Chandiramani, M.; Estarellas, C.; Frontera, A. *New J. Chem.* **2011**, *35*, 57−60. (v) Yang, Z.; Liu, Z.; Chen, Y.; Wang, X.; He, W.; Lu, Y. *Org. Biomol. Chem.* **2012**, *10*, 5073−5076.

(57) For recent reviews, see: (a) Ma, J.; Dasgupta, P. K. *Anal. Chim. Acta* **2010**, *673*, 117−125. (b) Xu, Z.; Chen, X.; Kim, H. N.; Yoon, J. *Chem. Soc. Rev.* **2010**, *39*, 127−137. (c) Jun, E. M.; Roy, B.; Ahn, K. H. *Chem. Commun.* **2011**, *47*, 7583−7601.

(58) Saki, N.; Dinc, T.; Akkaya, E. U. *Tetrahedron* **2006**, *62*, 2721−2725.